Chapter 6

Verification/Validation

Contents

6.1 Analysis of the Measurement Data

MATSTAB was validated against numerous stability measurements. Most measurements available are from the Forsmark site, since Forsmark does routinely measure stability during startup to check the newly loaded core. These operating points are very close to each other in power and core flow. Nevertheless, the data spans over ten years, during which period the fuel design changed dramatically. With very few exceptions, the results from MATSTAB compared very well with the measurements and/or RAMONA. Therefore, one conclusion is, that for the used fuel from ABB, Siemens and GE good model parameters are available and that the fuel type has no influence on the prediction quality of MATSTAB.

The people at Leibstadt handle things very differently. Stability tests are only conducted before or after major changes in the NPP, e.g. a power upgrade. In 1990 and 1993 very extensive stability measurements were conducted. These tests covered a wide range of operating points and global as well as regional oscillations were experienced.

As explained in Chapter 3.1.1 on page 25, the main difference between Leibstadt and Forsmark are the recirculation pumps. Leibstadt uses jet pumps driven by external pumps while Forsmark has internal pumps. Due to this difference and the occurrence of out-of-phase oscillations, the Leibstadt data is an important extension to the validation done for Forsmark.

After the successful application of MATSTAB for the above mentioned NPPs, the responsible people at Oskarshamn decided to compare MATSTAB results with their own stability investigations. The validation was conducted by Oskarshamn [19], therefore, we cannot present the results in the same detailed manner as for the other plants. Only decay ratios were compared. It is noteworthy, that the engineers at Oskarshamn were able to use MATSTAB efficiently after a short introduction to the program. The time needed to prepare the input data was short as well, since the POLCA distribution files and some RAMONA input files were available.

Table 6.1 gives a brief overview over the physical data of the different nuclear power plants involved in the validation of MATSTAB.

Naturally, the three above mentioned sites are not the only power plants conducting stability measurements. Due to restrictions in time, it was not possible to widen the validation basis, even though a validation against Ringhals measurements would have been very interesting. Nevertheless, the validation presented covers a large number of measurements and contains some of the most extreme measurements ever done for a commercial NPP (natural circulation in Leibstadt 1990). It remains to say, that the Leibstadt reactor is among the plants with the highest core power-density in the world.

One should always bear in mind, that the measurements have an uncertainty in decay ratio itself. Especially for well damped systems, different analysis tools lead to slightly different results. Even though there is a lot of instrumentation inside the plant, the state of the reactor is only known to a certain degree. Hence, the input to the computer codes is not precisely defined.

Plant	Power [MW]	Core Flow [kg/s]	Fuel Assemblies	Recirc. Pumps	Manufacturer
Forsmark 1	2700	11000	676	internal	ABB
Forsmark 2	2700	11000	676	internal	ABB
Forsmark 3	3020	11400	700	internal	ABB
Leibstadt	3138	11151	648	jet pumps	GE
Oskarshamn 1	1375	4600	448	external	ABB
Oskarshamn 2	1800	5100	444	external	ABB
Oskarshamn 3	3300	12000	700	internal	ABB

Table 6.1: Key Parameters of the NPPs Involved in Validating MATSTAB

Different people that attempt to predict the same measurement data may use a slightly different input and may obtain different decay ratios even if they use the same computer code (e.g. RAMONA 3.9 calculations from ABB, Forsmark, Vattenfall and Studsvik Scandpower). However, the differences lie more or less within +/- 0.05 in decay ratio. An OECD benchmark [34] for Ringhals showed calculation uncertainties that support this observation.

The frequency on the other side, is much less dependent on the state of the reactor and can be derived from the measurements with good accuracy. The predictions are normally very accurate and pose no problem, neither for the analysis of the measurements nor for the predictions of RAMONA and MATSTAB.

Not all signals from the many detectors within a NPP are normally recorded. Usually there are also capacity limits on how many non-standard signals may be recorded digitally with high resolution. For stability purposes LPRM (low power range monitor) detector signals are of high interest. The core of a normal BWR contains about 35 LPRM strings each containing four neutron detectors at four different axial heights. Normally about ten strings are selected and only one or two detector per string are recorded.

The frequency and the decay ratio of each operating point are commonly calculated from the measurements with an ARMA model [88], [35].

6.1.1 ARMA and ARMAX Models

The ARMAX (AutoRegressive Moving Average) technique interprets the fluctuations encountered in one signal $y(\tau)$ in terms of parameters of a linear model

$$y(\tau) = -\Sigma_{i=1}^{n_a} a_i * y(\tau - i) + \Sigma_{i=1}^{n_b} b_i * u(\tau - i) + \Sigma_{i=0}^{n_c} c_i * e(\tau - i) \tag{6.1}$$

which views $y(\tau)$ as responses to

- the fluctuations experienced in another signal $u(\tau)$, assumed to act as a systematic "driving source", plus
- an extra unknown disturbance $e(\tau)$ of an assumed "white" nature.

The model "parameters" in the vectors a, b and c are normally determined via a least-squares fitting procedure. The vectors obtained from the fitting can be interpreted in terms of a transfer function from the disturbing input $u(\tau)$ to the process $y(\tau)$.

The ARMA technique assumes that there is no systematic driving source; i.e. $u(\tau)$ is set to zero. The process fluctuations $y(\tau)$ are evaluated as though they were excited by the white noise $e(\tau)$ only.

For our purpose, the model orders (n_a, n_b) vary from 2 to 10 and the model which predicts the highest decay ratio in the frequency window of 0.3Hz - 0.7Hz is chosen.

Comprehensive functions to generate and use ARMAX models are provided by the system identification tool-box of MATLAB.

A recommendable textbook about system identification and the modeling of dynamic systems was written by Ljung [47].

6.1.2 Comparing LPRM Signals With MATSTAB

In addition to validate against decay ratio and frequency, the MATSTAB calculation may also be compared directly with a LPRM detector signal. A possibly existing linear trend is first removed from the time series of the detector, so that the signal is oscillating around the zero axis. As described above, the dominating frequency in the range of 2-4 rad/s is calculated. Using this frequency and a reference signal (e.g. APRM A), an ARMAX model is used to calculate the relative phase and amplitude of the original signal. This procedure is repeated for all the LPRM detector signals available. The same physical properties are taken directly from the right eigenvector of the MATSTAB solution. Since the detector position may be somewhere between the center of two core nodes, the values are linearly interpolated between the neighboring core nodes.

In the Figures (6.5-6.10) the phases and amplitudes from the measurement and the calculation are compared with each other. The measurements are represented by white vectors, the

calculations are represented by black vectors. Since the phase and amplitude of the MATSTAB vectors are only defined relatively to each other, the largest amplitude of the MATSTAB vectors is used to scale the LPRM signal vectors (the other way round would be more logical, but this way round the size of the vectors fits better into the plot). Hence one white and one black vector is always in perfect agreement. As a result, one vector would not be visible on the plot. This is slightly disturbing for the impression of the plot and therefore the vector is shown with a slight deviation to be visible nevertheless.

6.2 Global Oscillations

Since most of the measurements were done during normal start up, the measured decay ratios are quite small and relate to global oscillations. Some comparisons with regional oscillations follow in the next section, where the Leibstadt data from 1990 is investigated.

6.2.1 Forsmark

MATSTAB was validated against 42 stability measurements conducted in the cycles 8-19 at the Forsmark NPP in Sweden [109],[110],[111]. The range of operating points lay between 3800 and 5000 kg/s of core flow and 59% to 68% power (see Tables 6.2, 6.3 and 6.4).

Forsmark 1

MATSTAB was validated against 18 stability measurements Forsmark 1 conducted in the cycles 10-19. The range of operating points lay between 3800 and 4400 kg/s of core flow and 59% to 66% power. Table 6.2 summarizes the results and shows a good agreement between MATSTAB and the measurement. The abbreviation boc/moc/eoc are used to describe beginning/middle/end of cycle, whereas aug stands for august.

Only three calculated decay ratios differ more than 0.1 from the measurement, and most of them are much closer (Figures 6.1, 6.2). The standard deviation for all cases is 0.06 for the decay ratio and 0.02 for the frequency.

The available RAMONA 3.9 calculations [105], [33] are included in the table to show that MATSTAB and RAMONA are of comparable accuracy, despite the linearized equations used in MATSTAB (Figure 6.3, 6.4). The standard deviation of the RAMOMA runs is also 0.05 for the decay ratio. However, if only the measurements where RAMONA runs are available are evaluated, MATSTAB reaches a standard deviation of 0.05 as well.

The content of Figures 6.5-6.10 are explained in Section 6.1.2 and Chapter 5. They basically show the part of the right eigenvector which relates to the thermal neutron flux (colors) and the comparison between the measured and the calculated LPRM oscillation (arrows). The agreement between the white (measurement) and black (calculation) arrows is reasonably well. Especially the angle (phase-shift) between the arrows is predicted correctly.

Operating point			Decay Ratio			Frequency [Hz]		
Cycle	Power [%]	Core Flow [Kg/s]	Measurement	MATSTAB	RAMONA 3.9	Measurement	MATSTAB	RAMONA 3.9
c10 boc	65.5	4100	0.49	0.60		0.47	0.45	
c11 boc	65.2	3966	0.46	0.45		0.44	0.41	
c12 boc	64.5	4183	0.53	0.51		0.49	0.45	
c13 boc 1	59.6	3987	0.40	0.38	0.43	0.45	0.42	0.44
c13 boc 2	59.9	4317	0.30	0.28	0.30	0.46	0.42	0.45
c13 boc 3	64.3	4385	0.49	0.43	0.38	0.48	0.45	0.48
c13 boc 4	65.1	4044	0.68	0.52		0.47	0.44	
c14 boc 1	59.9	4383	0.44	0.36	0.38	0.49	0.44	0.45
c14 moc 2	64.3	4092	0.60	0.48	0.58	0.48	0.43	0.47
c14 boc 3	64.8	4313	0.56	0.51	0.53	0.51	0.46	0.48
c14 boc 4	64.7	4014	0.64	0.56	0.66	0.51	0.46	0.47
c15 boc	64.4	4057	0.63	0.57	0.56	0.53	0.48	0.46
c15 aug	64.1	4027	0.38	0.37		0.45	0.42	
c17 boc	65.0	3940	0.40	0.41	0.34	0.45	0.45	
c17 eoc	64.5	3823	0.58	0.52		0.45	0.45	
c18 boc	64.7	4043	0.56	0.62	0.42	0.55	0.52	
c18 moc	62.6	4045	0.44	0.45	0.46	0.46	0.46	
c19 boc	63.7	3884	0.61	0.59		0.52	0.50	

Table 6.2: Comparison Between MATSTAB and Measurements in Forsmark 1

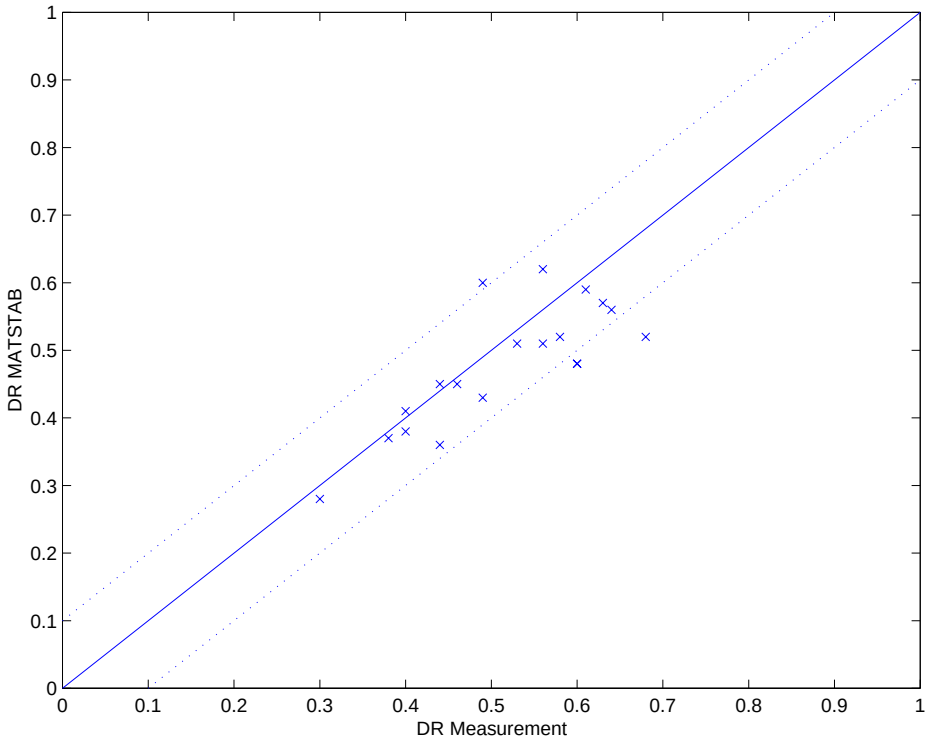

Figure 6.1: Validation of the Decay Ratio for Forsmark 1

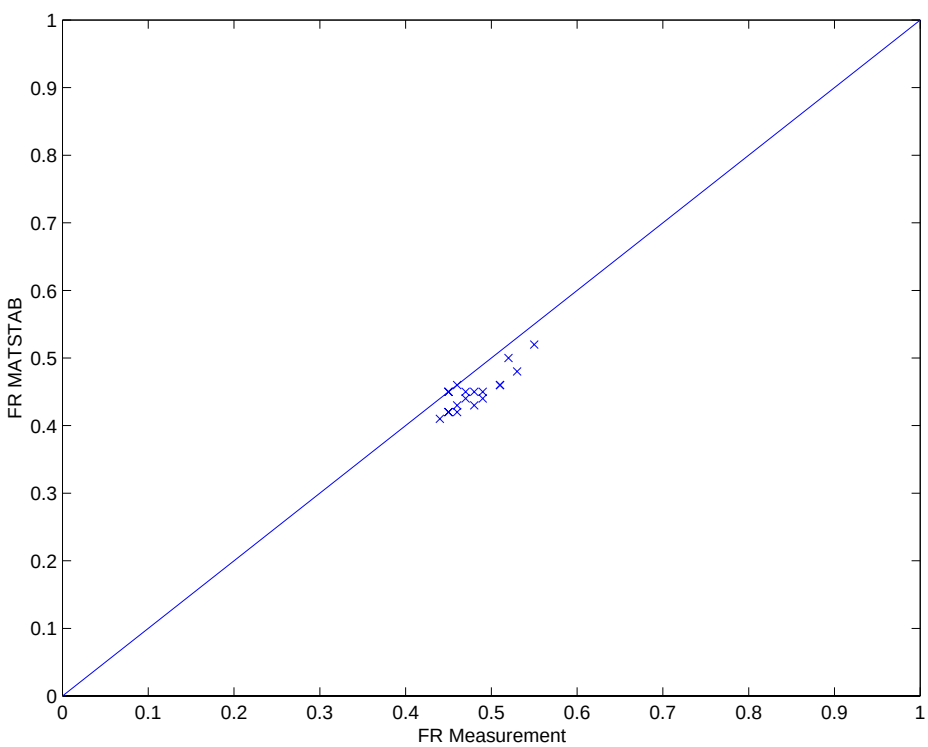

Figure 6.2: Validation of the Frequency for Forsmark 1

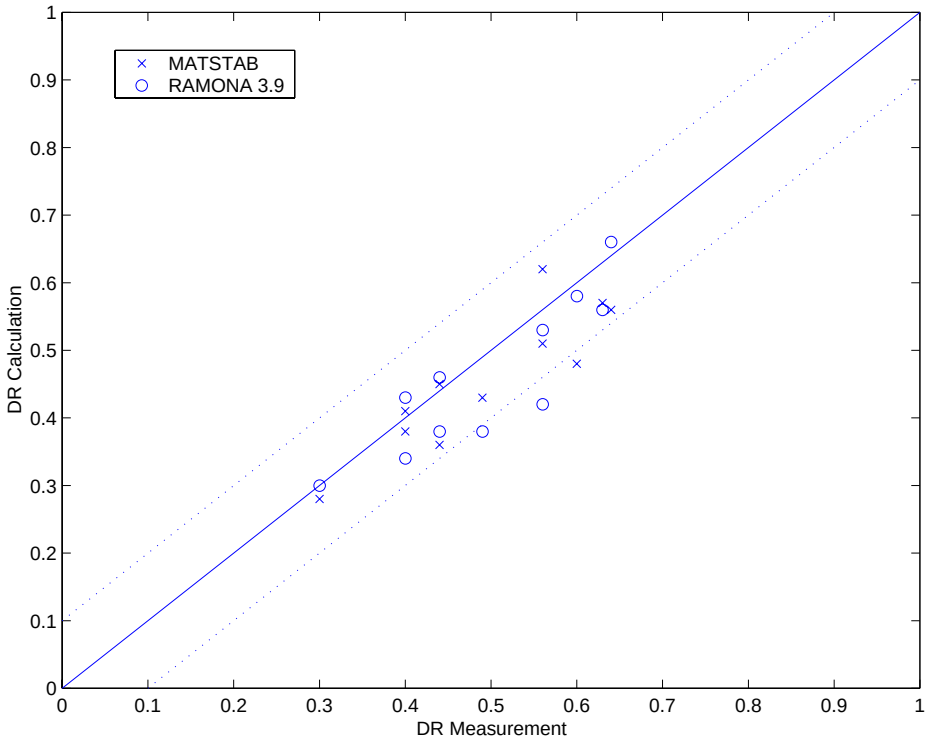

Figure 6.3: Comparison Measurement/MATSTAB/RAMONA 3.9 for Forsmark 1

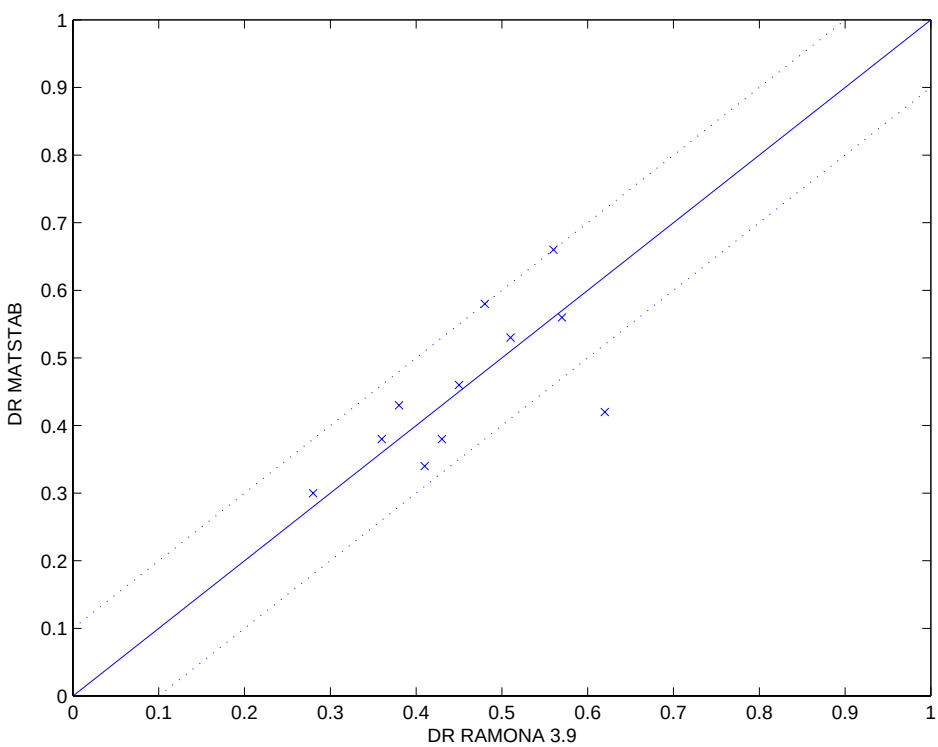

Figure 6.4: Comparison of MATSTAB and RAMONA 3.9 for Forsmark 1

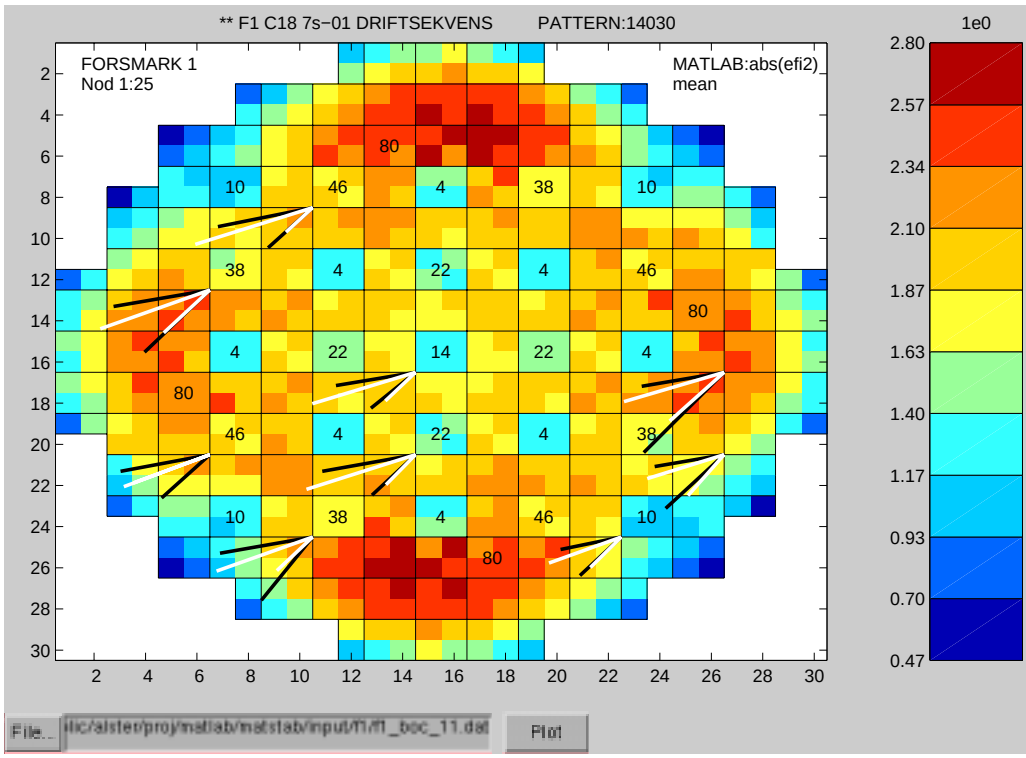

Figure 6.5: Comparison of MATSTAB and Measurement C11 boc in Forsmark 1

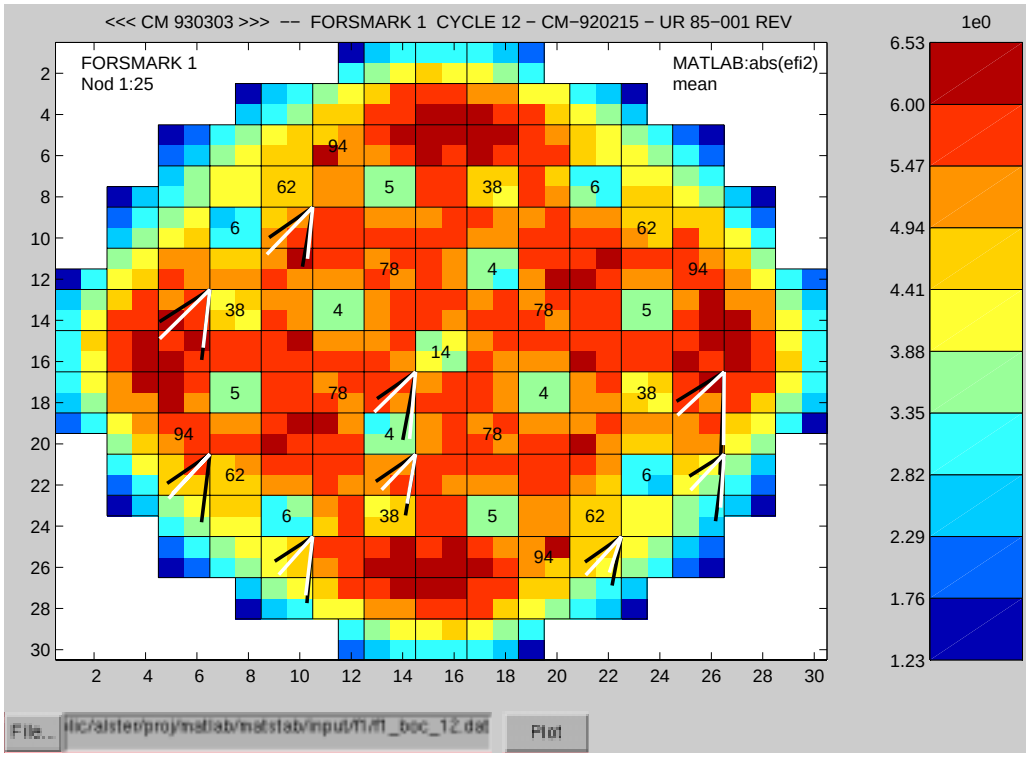

Figure 6.6: Comparison of MATSTAB and Measurement C12 boc in Forsmark 1

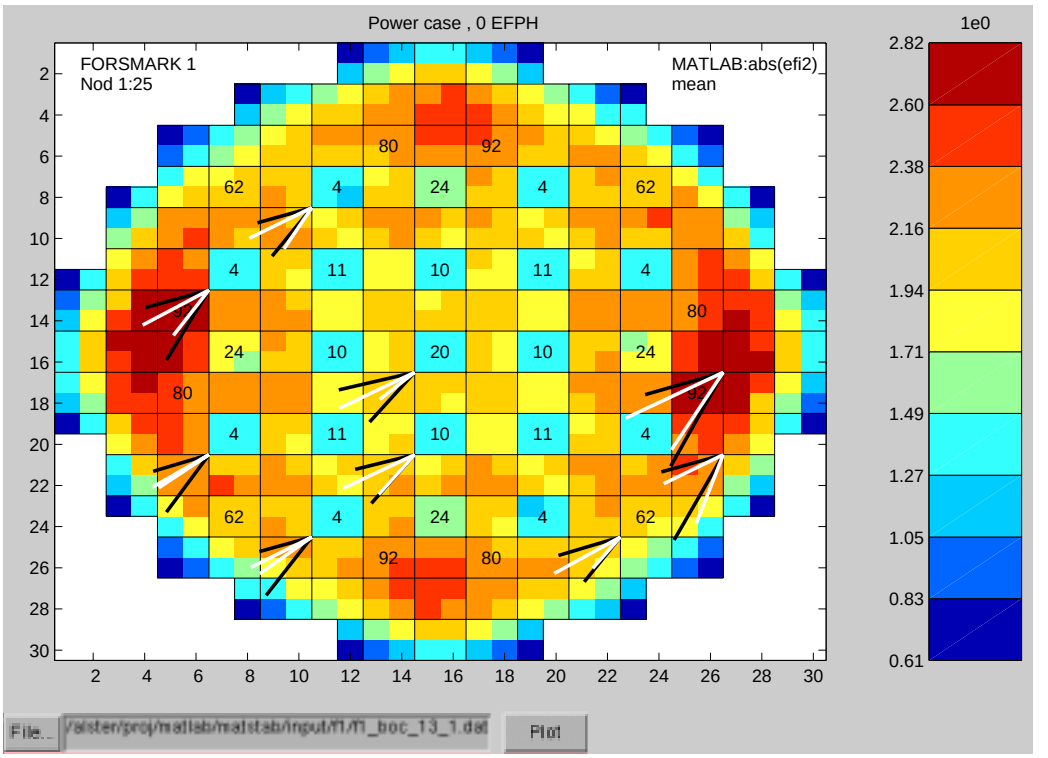

Figure 6.7: Comparison of MATSTAB and Measurement C13-1 boc in Forsmark 1

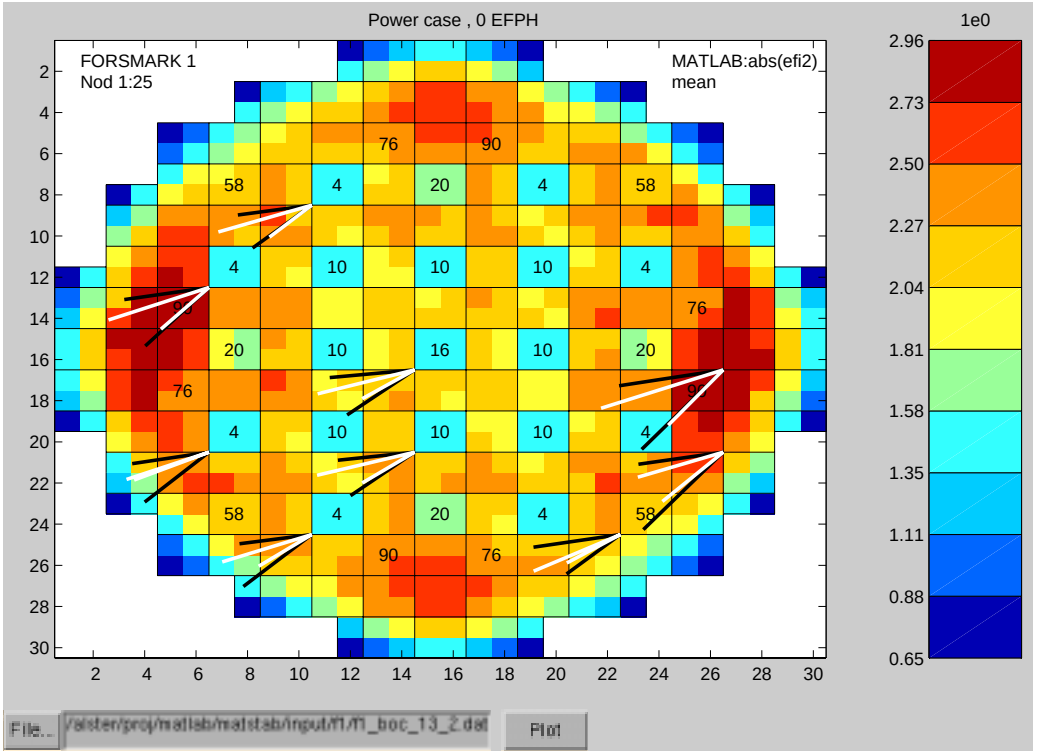

Figure 6.8: Comparison of MATSTAB and Measurement C13-2 boc in Forsmark 1

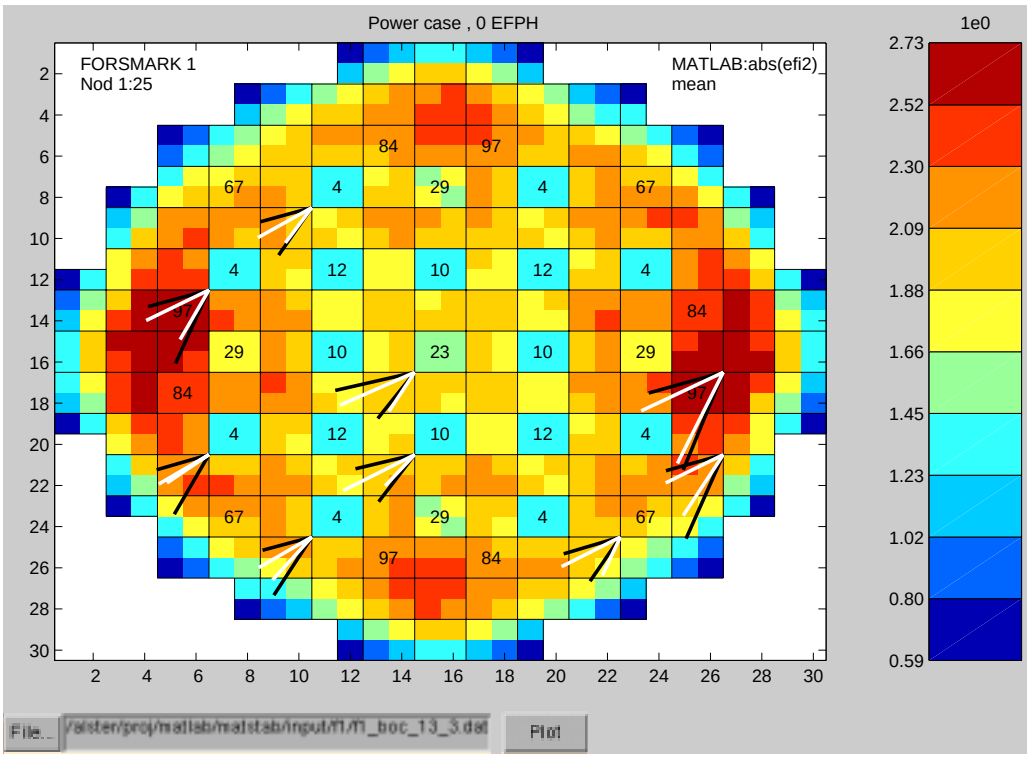

Figure 6.9: Comparison of MATSTAB and Measurement C13-3 boc in Forsmark 1

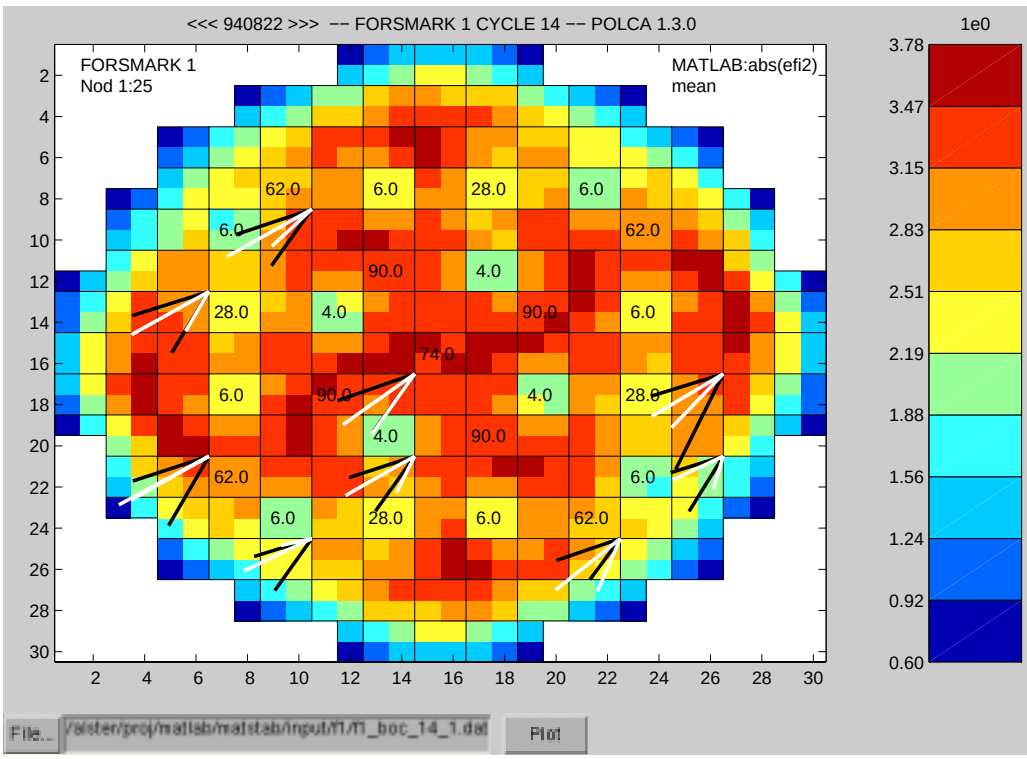

Figure 6.10: Comparison of MATSTAB and Measurement C14-1 boc in Forsmark 1

Forsmark 2

MATSTAB was validated against 11 stability measurements Forsmark 2, conducted in the cycles 12-17. The range of operating points lay between 3800 and 4200 kg/s of core flow and 60% to 70% power (see Table 6.3). The standard deviation for all cases is 0.09 for the decay ratio and 0.03 for the frequency. The newly released code RAMONA 5 was validated against some of the Forsmark 2 measurements [44]. The results are also printed in Table 6.3 to show that even the improved RAMONA code does not deliver better results than MATSTAB. Actually, RAMONA 5 shows at the moment worse results than RAMONA 3.9. The standard deviation for the decay ratio is 0.13.

Operating point			Decay Ratio			Frequency [Hz]	
Cycle	Power [%]	Core Flow [Kg/s]	Measurement	MATSTAB	RAMONA 5	Measurement	MATSTAB
c12 boc	65.0%	4083	0.46	0.48		0.44	0.42
c13 moc	64.3%	3940	0.52	0.51		0.40	0.41
c14 startup	65.1%	4028	0.52	0.55	0.56	0.43	0.43
c14 boc	65.0%	4026	0.46	0.50		0.47	0.44
c14 moc	63.3%	3850	0.73	0.47	0.60	0.47	0.37
c15 startup	64.0%	3791	0.49	0.40	0.64	0.40	0.36
c15 moc	67.3%	4234	0.68	0.69	0.57	0.49	0.49
c16 boc	64.0%	4127	0.69	0.66	0.56	0.48	0.48
c17 boc	64.4%	3948	0.30	0.38	0.53	0.41	0.41
c17 2300	64.3%	3896	0.60	0.52	0.61	0.46	0.43
c17 moc	62.6%	3980	0.68	0.66	0.71	0.45	0.46

Table 6.3: Comparison Between MATSTAB and Measurements in Forsmark 2

Figure 6.11 and 6.12 compare the MATSTAB calculations with the values obtained from the measurements.

If the measurement of cycle 14 moc is omitted, the deviation of MATSTAB is only 0.05 for the decay ratio respectively 0.02 for the frequency. The RAMONA 5 results, however, do not benefit in the same way from the omission of 14 moc. The standard deviation stays the same.

Figure 6.15 shows, that the difference between the measurement and the calculations of MATSTAB is larger for low core flows than it is for high flows. The reason lies in the model for the recirculation pumps. This effect is studied in [108].

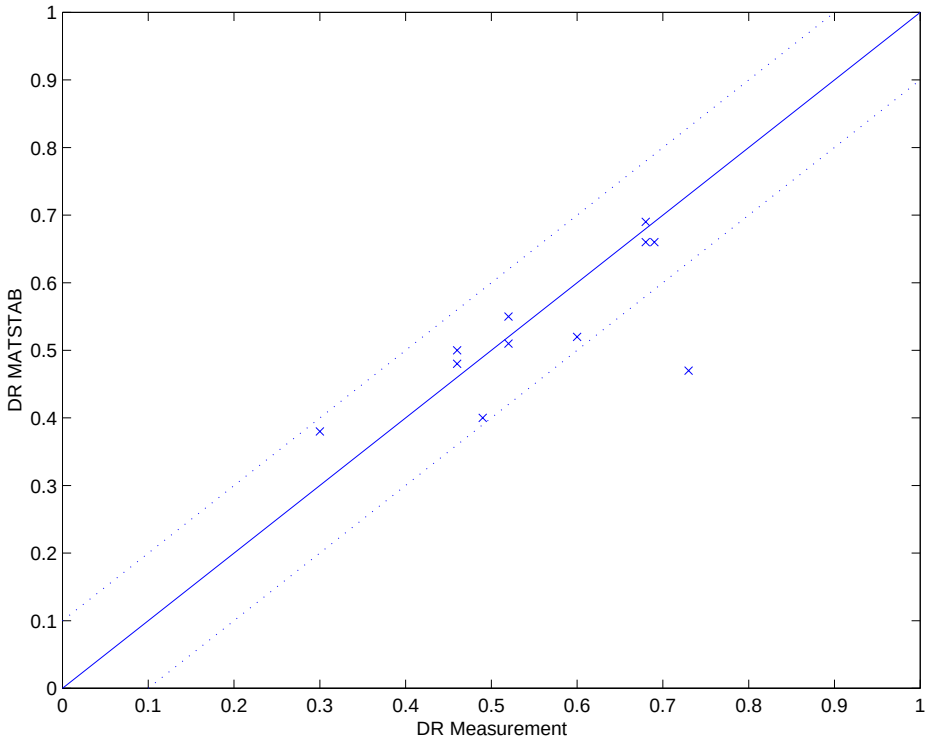

Figure 6.11: Validation of the Decay Ratio for Forsmark 2

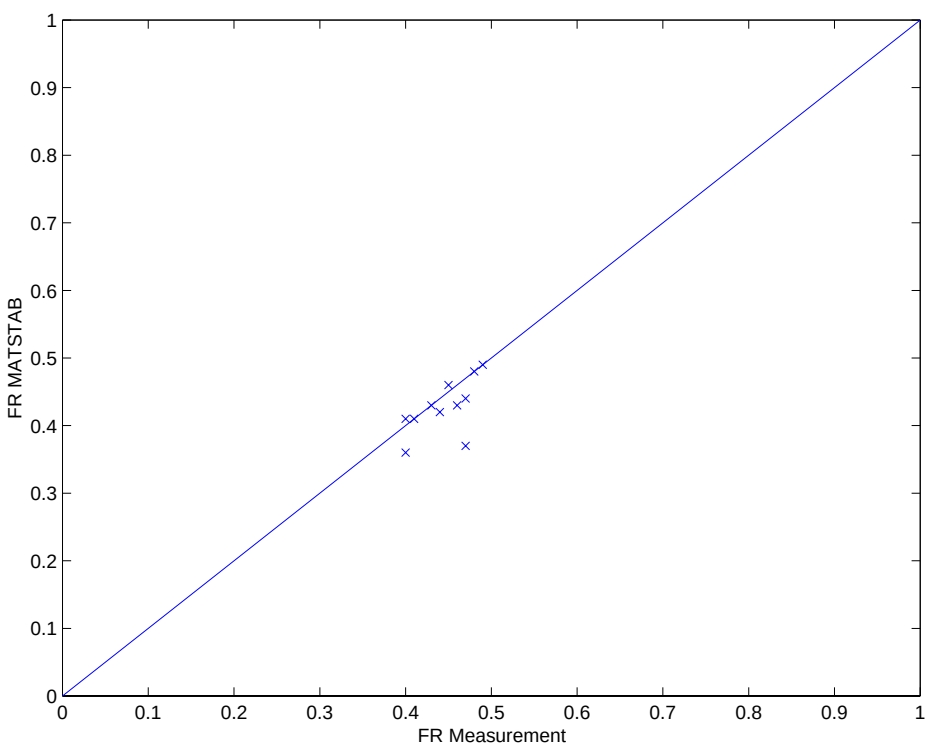

Figure 6.12: Validation of the Frequency for Forsmark 2

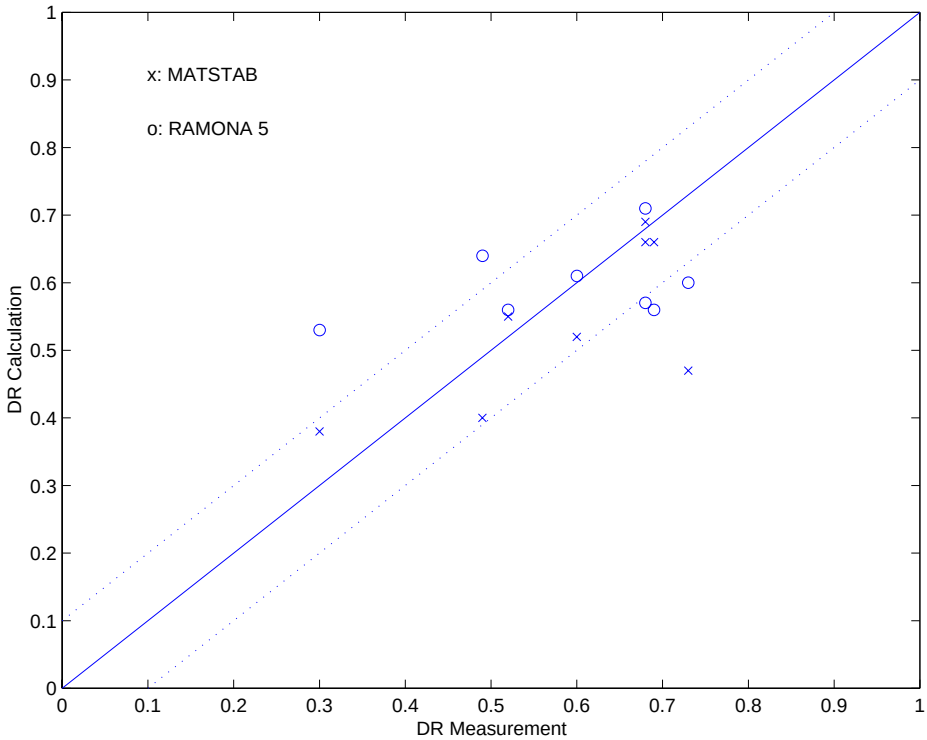

Figure 6.13: Comparison Measurement/MATSTAB/RAMONA 5 for Forsmark 2

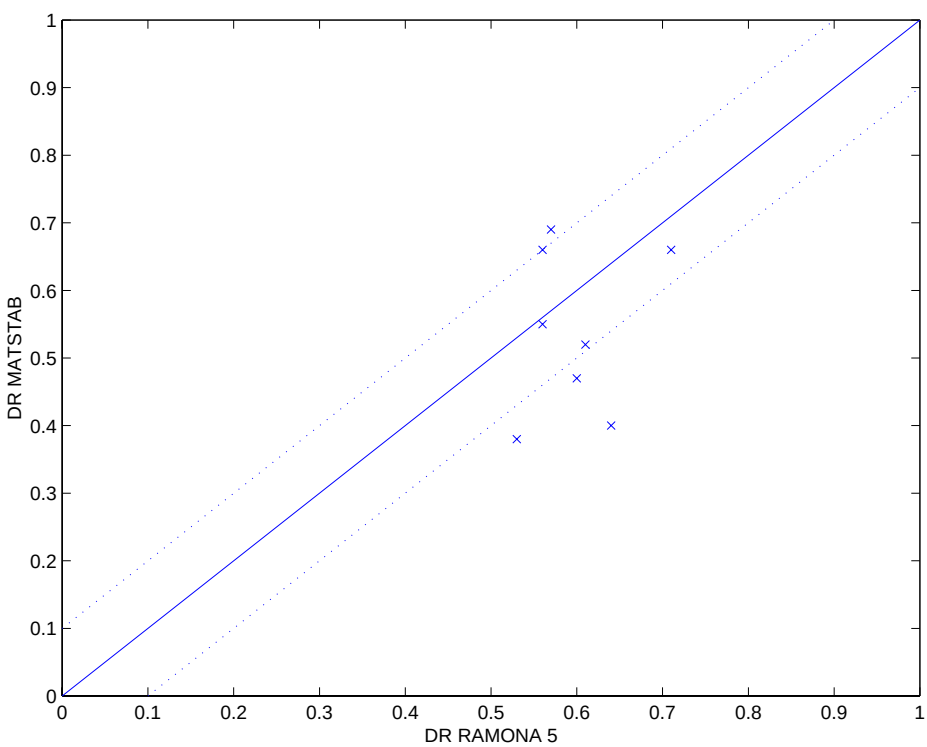

Figure 6.14: Comparison of MATSTAB and RAMONA 5 for Forsmark 2

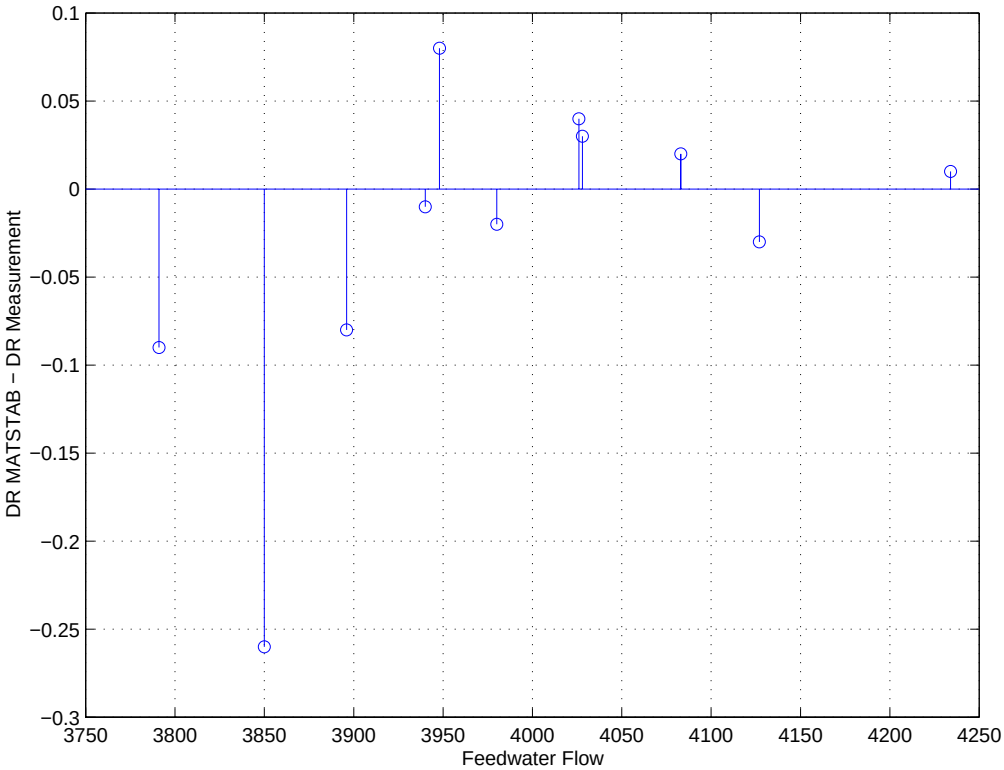

Figure 6.15: Comparison Measurement/MATSTAB with Respect to the Core Flow

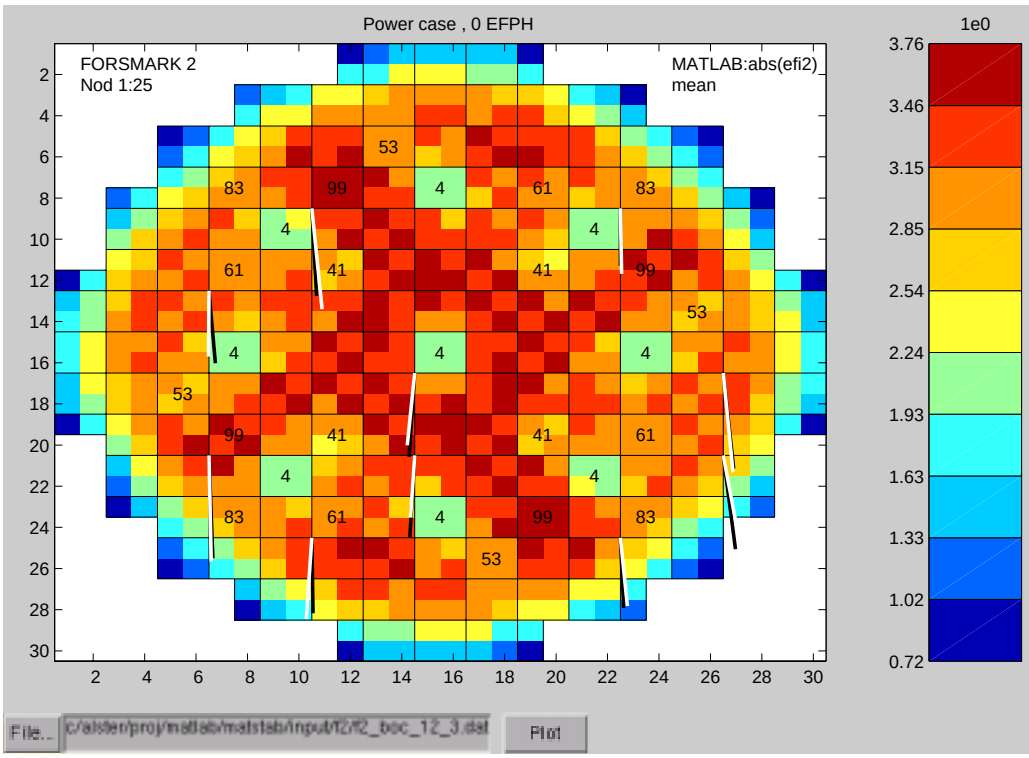

Figure 6.16: Comparison of MATSTAB and Measurement C12 boc in Forsmark 2

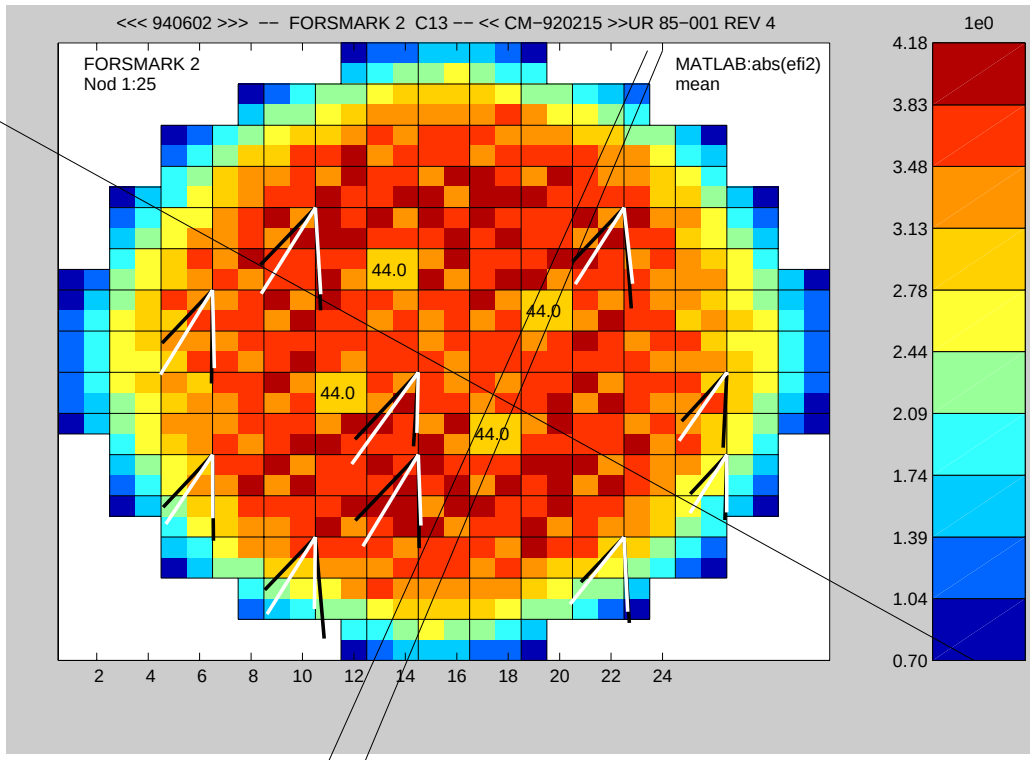
<<< 940602 >>> -- FORSMARK 2 C13 -- << CM-920215 >>UR 85-001 REV 4
FORSMARK 2
Nod 1:25
MATLAB:abs(efi2)
mean
1e0
4.18
3.83
3.48
3.13
2.78
2.44
2.09
1.74
1.39
1.04
0.70
44.0
44.0
44.0
44.0
2
4
6
8
10
12
14
16
18
20
22
24

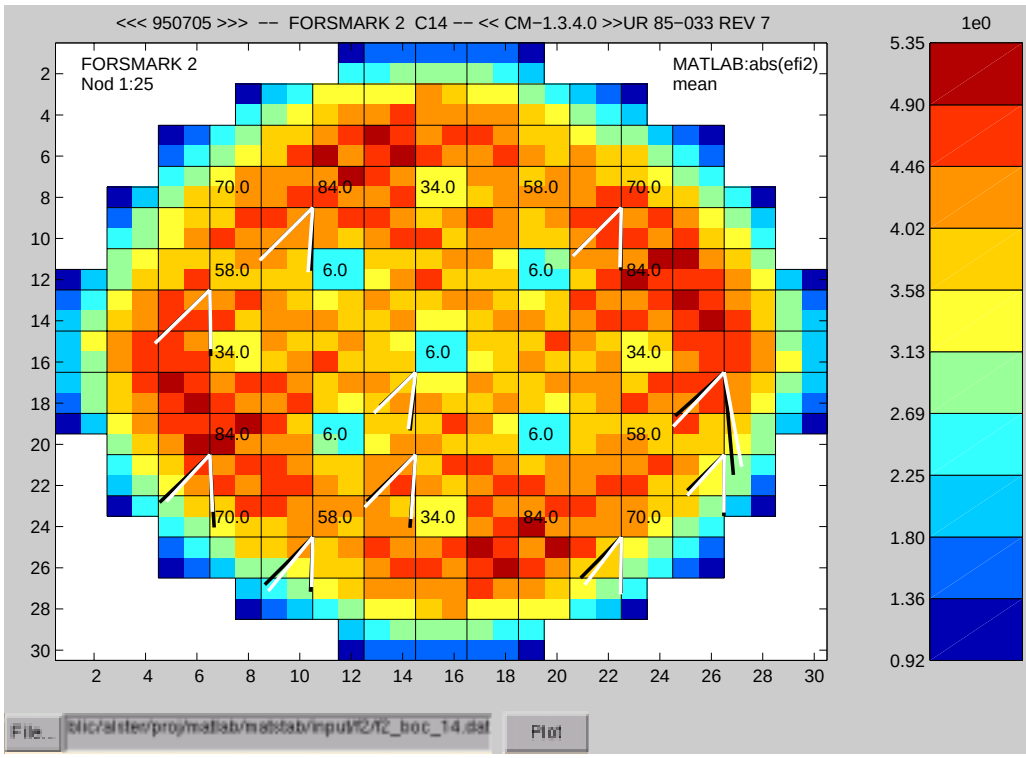

Figure 6.19: Comparison of MATSTAB and Measurement C14 boc in Forsmark 2

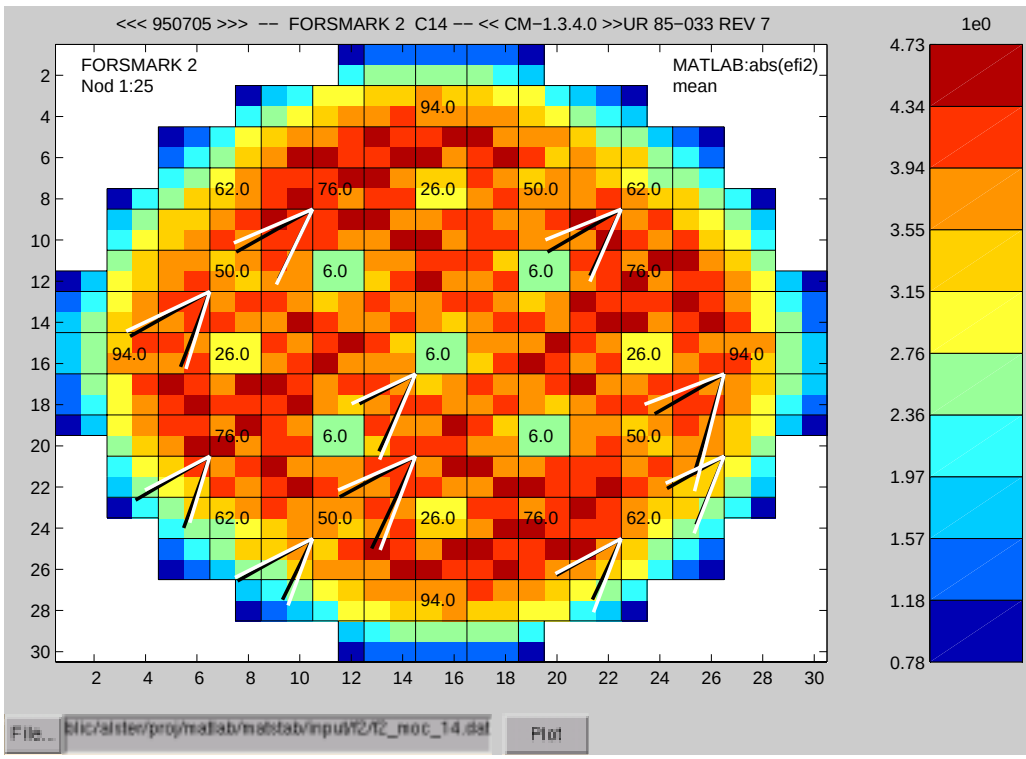

Figure 6.20: Comparison of MATSTAB and Measurement C14 moc in Forsmark 2

The content of Figures 6.16-6.20 are explained in Section 6.1.2 and Chapter 5. The agreement between measured and calculated LPRM signal oscillations for Forsmark 2 is even better than the agreement for Forsmark 1, especially cycle 14 yields very good results.

Forsmark 3

MATSTAB was validated against 13 stability measurements Forsmark 3 conducted in the cycles 8-14. The range of operating points lay between 4200 and 5000 kg/s of core flow and 63% to 66% power (see Table 6.3).

Operating point			Decay Ratio		Frequency [Hz]	
Cycle	Power [%]	Core Flow [Kg/s]	Measurement	MATSTAB	Measurement	MATSTAB
C8 boc	63.0	4218	0.48	0.47	0.48	0.44
C8 moc	65.0	4533	0.70	0.69	0.50	0.49
C9 boc	65.0	4300	0.58	0.48	0.48	0.46
C9 moc	65.0	4240	0.76	0.75	0.54	0.51
C10 boc	64.9	4275	0.52	0.55	0.47	0.51
C10 moc	63.6	4756	0.50	0.56	0.52	0.52
C12 boc	64.6	4644	0.50	0.51	0.47	0.50
C12 moc	63.2	4965	0.44	0.51	0.51	0.54
C13 boc	64.0	4600	0.45	0.44	0.44	0.46
C13 moc	63.8	4535	0.55	0.62	0.51	0.52
C14 boc	63.7	4168	0.51	0.52	0.46	0.45
C14 nov	62.2	4799	0.52	0.47	0.49	0.49
C14 jan	65.1	4820	0.52	0.58	0.50	0.49

Table 6.4: Comparison Between MATSTAB and Measurements in Forsmark 3

Figure 6.21 and 6.22 compare the MATSTAB calculation with the values obtained from the measurement. The standard deviation for all cases is 0.05 for the decay ratio and 0.02 for the frequency.

Figures 6.23 - 6.28 show again good agreement between calculated and measured LPRM signal oscillations. Even for detector strings with four LPRM detectors, the phase-shift is predicted well.

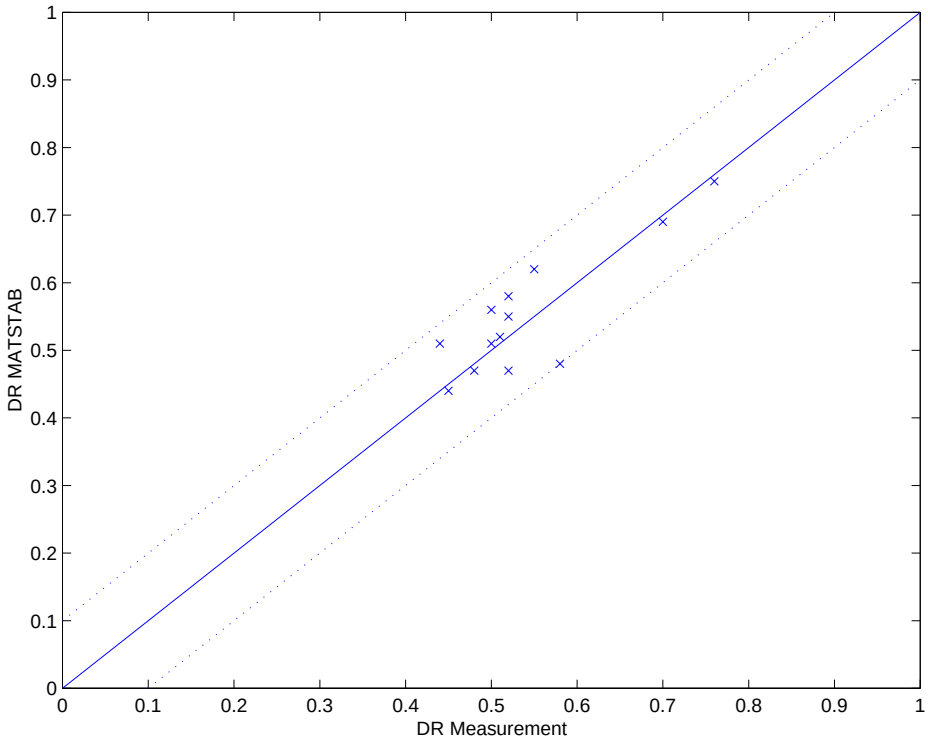

Figure 6.21: Validation of the Decay Ratio for Forsmark 3

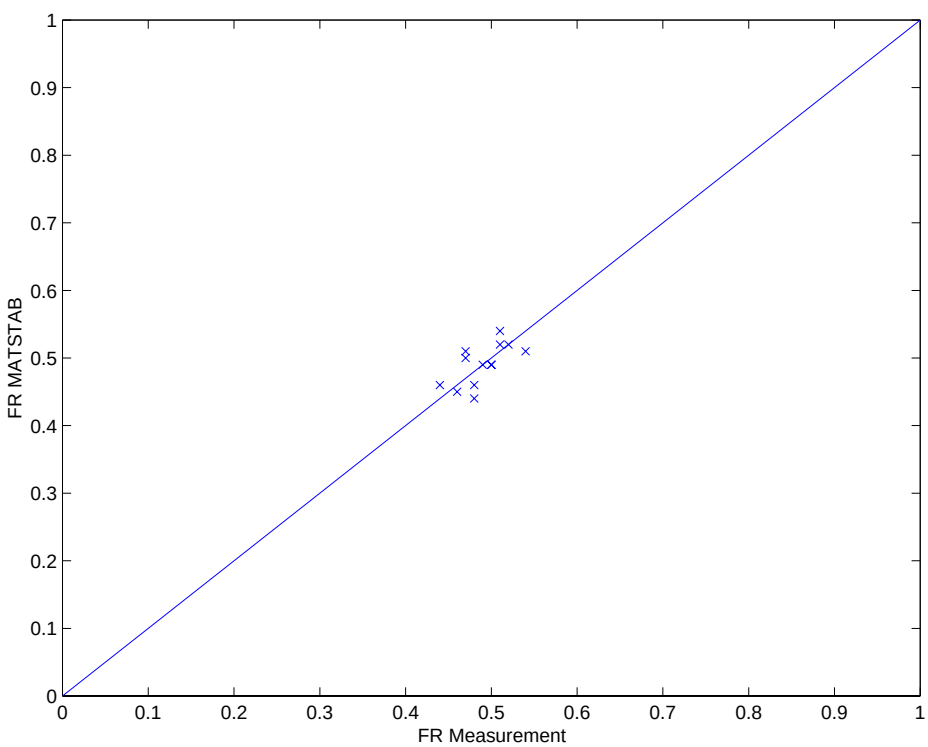

Figure 6.22: Validation of the Frequency for Forsmark 3

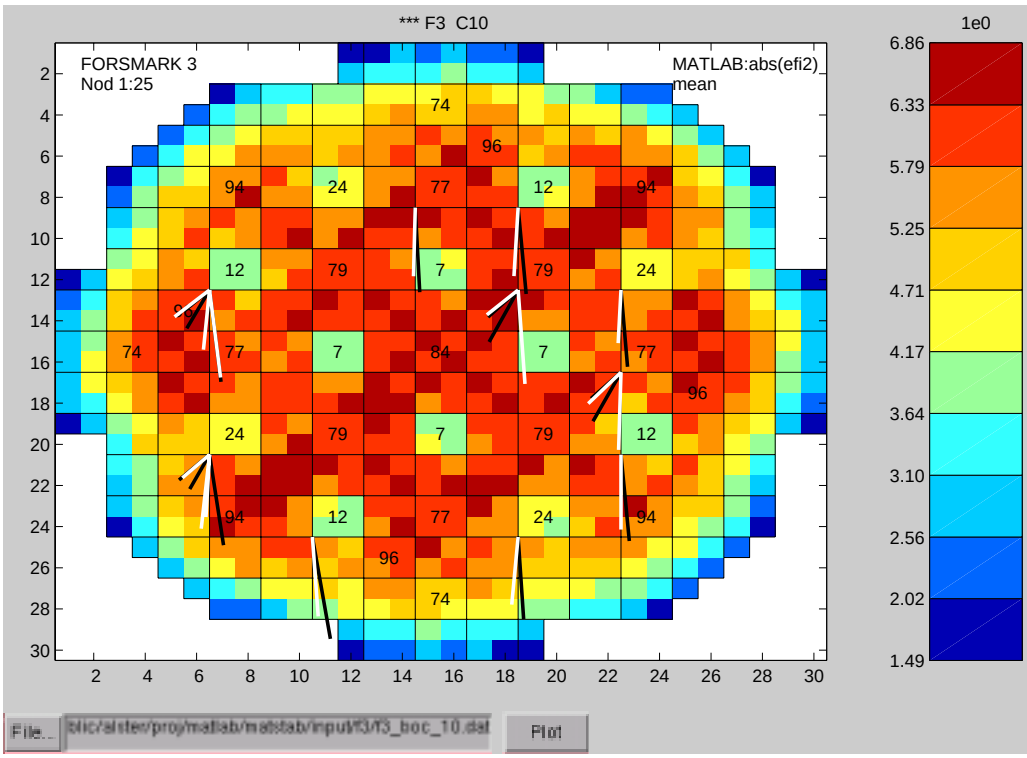

Figure 6.23: Comparison of MATSTAB and Measurement C10 boc in Forsmark 3

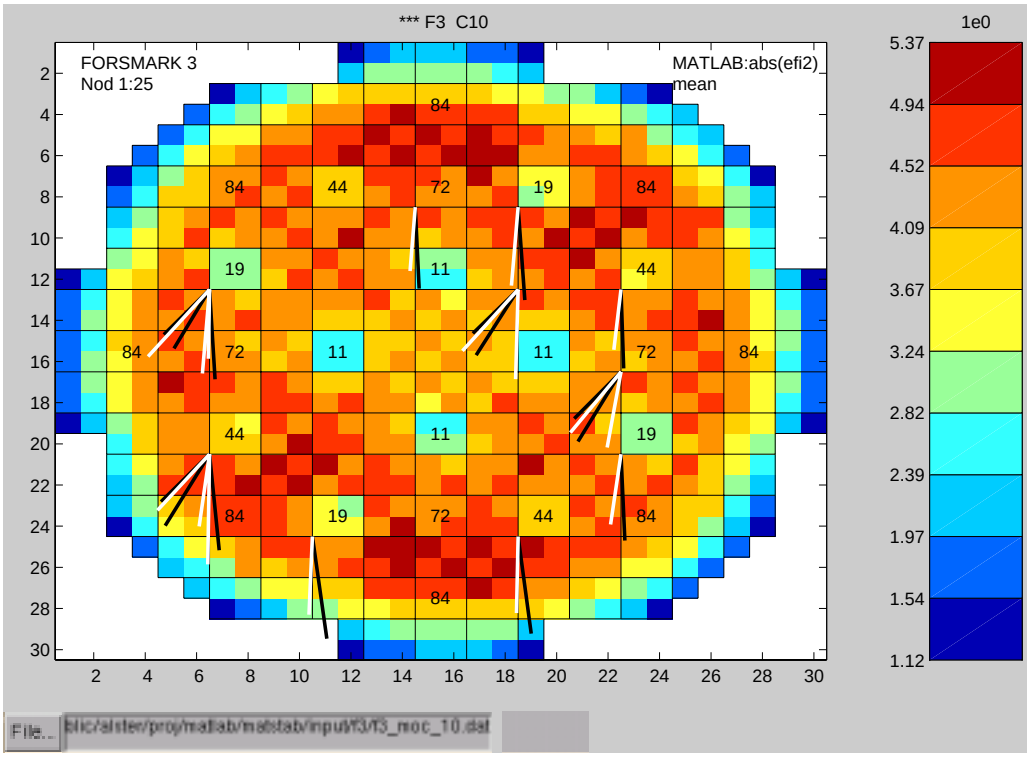

Figure 6.24: Comparison of MATSTAB and Measurement C10 moc in Forsmark 3

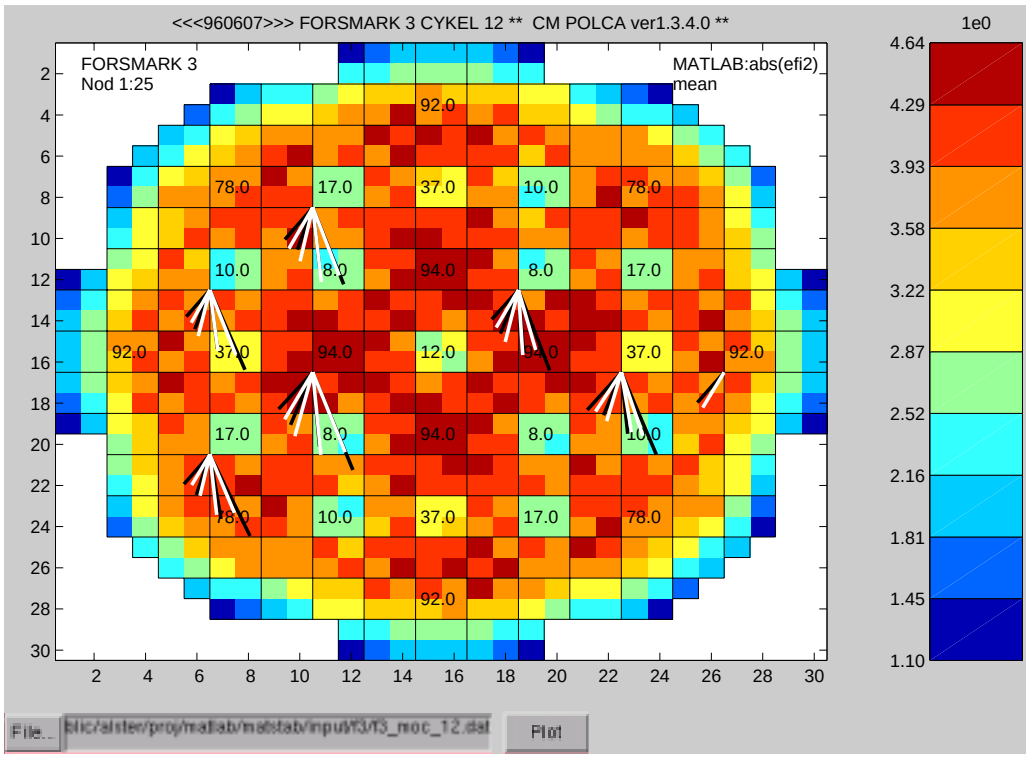

Figure 6.25: Comparison of MATSTAB and Measurement in C12 moc Forsmark 3Fi gure

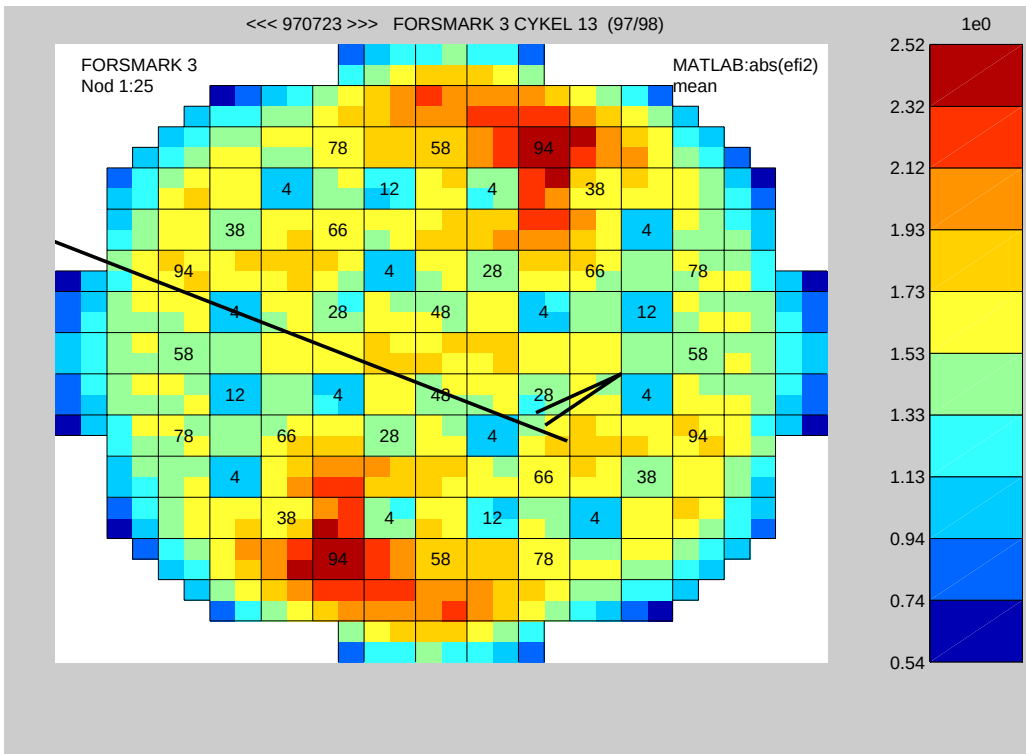


4.33
4.00
3.66
3.33
2.99
2.66
2.32
1.99
1.66
1.32
0.99

6.2.2 Oskarshamn

All the following results are taken from the MATSTAB validation report [19] prepared by Oskarshamn. The information is added to show that MATSTAB gives good results for NPPs which it was not tested against during the development phase. It is also noteworthy, that the Oskarshamn people had no problems with generating the input desks for MATSTAB or using the code in general.

Operating point			Decay Ratio			Operating point			Decay Ratio	
Cycle	Power [%]	Core Flow [Kg/s]	Measurement	MATSTAB		Cycle	Power [%]	Core Flow [Kg/s]	Measurement	MATSTAB
Oskarshamn 1						Oskarshamn 3				
C21	75.1	2767	0.35	0.37		C10	74.7	6399	0.31	0.46
C21	75.1	2889	0.32	0.29		C10	59.8	4384	0.67	0.70
C22	74.0	2776	0.27	0.35		C10	56.4	4090	0.71	0.66
C23	74.3	2797	0.24	0.32		C10	60.2	4354	0.77	0.75
C24	75.4	2747	0.44	0.46		C11	63.4	4425	0.72	0.76
C24	74.5	2724	0.48	0.42		C11	60.5	4380	0.70	0.76
						C12	62.7	4360	0.68	0.74
Oskarshamn 2						C12	62.5	4360	0.83	0.75
C19	85.0	3175	0.60	0.69		C13	65.3	4796	0.69	0.70
C19	82.4	2966	0.64	0.74		C13	60.5	4177	> 1	1.00
C19	78.9	2949	0.69	0.64		C13	65.0	5100	0.63	0.50
C19	83.6	3172	0.73	0.65		C14	50.0	4978	0.32	0.26
C19	80.8	3003	0.60	0.69		C14	50.0	5344	0.30	0.22
C19	78.8	2995	0.67	0.63		C14	66.2	5083	0.60-0.63	0.54
C20	80.1	2966	0.58	0.53		C14	66.0	5000	0.56-0.63	0.57
C20	81.5	3005	0.62	0.67		C14	66.8	5400	0.47	0.43
C20	79.1	3052	0.58	0.61		C14	66.2	5122	0.67	0.54
C21	91.3	2993	0.62	0.57		C14	67.0	5375	0.67	0.52
C21	78.3	3036	0.47	0.53		C15	75.0	6240	0.54	0.35
C22	82.8	3024	0.57	0.50		C15	71.0	6040	0.45	0.35
C23	70.8	2630	0.38	0.45						
C23	83.7	3186	0.50	0.46						
C24	85.1	3180	0.53	0.43						
C25	73.3	2991	0.42	0.50						

Table 6.5: Comparison Between MATSTAB and Measurements in Oskarshamn

Oskarshamn 1

MATSTAB shows good agreement with the measurements of Oskarshamn 1 (Figure 6.29) even though the decay ratios in general are very small. The standard deviation for all cases is 0.06 for the decay ratio.

Oskarshamn 2

MATSTAB shows good agreement with the measurements of Oskarshamn 2 (Figure 6.30). In cycle 19-20 the core contained only SVEA-64 fuel assemblies. In cycle 21-24 Atrium-9 fuel was introduced, in cycle 24 and 25 Atrium-10B. The partial length rods introduced with the new fuel types lead to no problems for the 3D neutronics of MATSTAB. The measurement data from Oskarshamn 2 is taken from the online stability monitor and not from a thorough investigation of the LPRM data. This may be a reason for the slightly higher deviations when compared with Oskarshamn 1. The standard deviation is 0.07 in decay ratio.

Oskarshamn 3

MATSTAB shows good agreement with the measurements of Oskarshamn 3 up till cycle 13 (Figure 6.31). In cycle 14 the deviation is large and in cycle 15 the deviation is unreasonably large. The reason for the large error in the latest two cycles is not yet understood. The standard deviation of all measurements is 0.08 for the decay ratio.

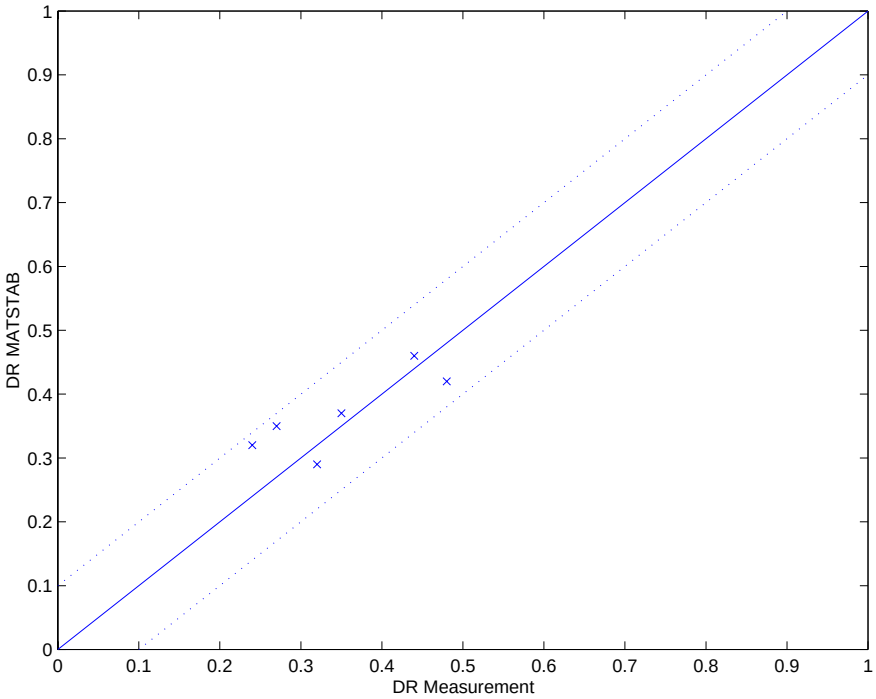

Figure 6.29: Validation of the Decay Ratio for Oskarshamn 1

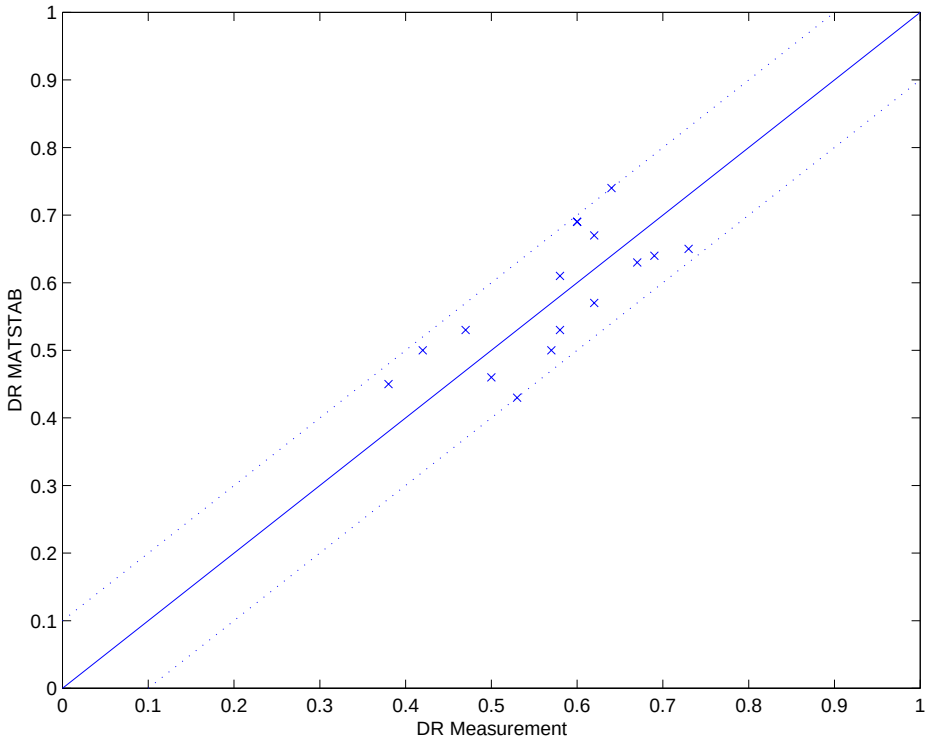

Figure 6.30: Validation of the Decay Ratio for Oskarshamn 2

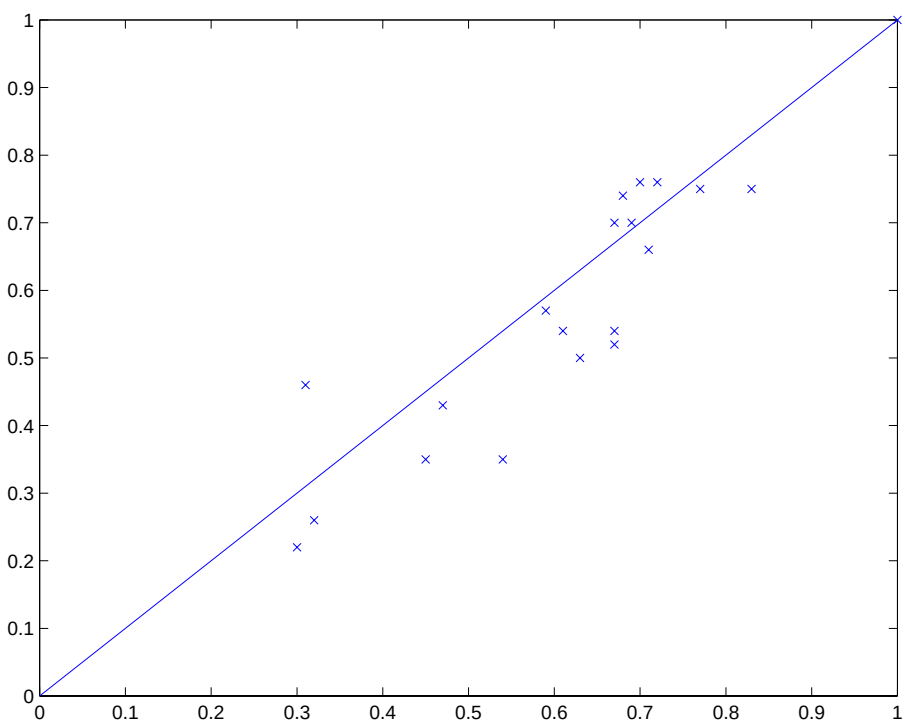

6.2.3 Leibstadt

A core stability test was conducted in KKL shortly after the beginning of cycle ten (see [86] or Chapter 5 for an extensive analysis). The core contained about 51% of 10x10 lattice SVEA-96 fuel. The remainder consisted chiefly of 8x8 lattice GE-8 and GE-10 fuel. The range of operating points lay between 3050 and 7784 kg/s of core flow and 45% to 77% power (see Table 6.6). As for the Forsmark and Oskarshamn cases, MATSTAB is able to predict the decay ratios and frequencies with reasonable accuracy. The standard deviation for all cases is 0.08 for the decay ratio and 0.02 for the frequency.

Operating point			Decay Ratio			Frequency [Hz]		
Cycle	Power [%]	Core Flow [Kg/s]	Measurement	MATSTAB global	MATSTAB regional	Measurement	MATSTAB global	MATSTAB regional
C10	77	7784	0.22	0.07	0.09	0.63	0.60	0.66
C10	68	5078	0.44	0.42	0.46	0.60	0.52	0.57
C10	61	4464	0.53	0.56	0.57	0.54	0.47	0.52
C10	59	4010	0.65	0.65	0.65	0.50	0.44	0.48
C10	45	3050	0.97	1.02	1.03	0.47	0.42	0.45

Table 6.6: Comparison Between MATSTAB and Measurements in Leibstadt

Figures 6.32 and 6.33 compare the global mode of the MATSTAB calculation with the values obtained from the measurements. If the first operating point is omitted (the DR of very stable points is extremely hard to predict though not important for the analysis), the standard deviation is 0.03 for the decay ratio and 0.02 for the frequency.

In contrast to the measurement series in cycle seven, which is discussed later, neither the online monitoring system nor the post analysis indicated the appearance of regional oscillations. However, MATSTAB predicts a significant possibility for regional oscillations in the cycle ten measurements series. The global and the regional modes have decay ratios of similar size and correspond to the decay ratios measured during the experiment. Actually, the regional decay ratios are slightly larger than the global ones (see Table 6.6). Interestingly, the frequencies of the regional oscillations are in general closer to the measurement than the frequencies from the global oscillations. Assuming that the MATSTAB calculations are correct, it is astonishing, that in none of the five operating points the slightest indication for regional oscillation were seen. One explanation is, that the signal amplitude of the regional oscillation was much smaller than the signal amplitude of the global oscillation. This would make it difficult to detect the regional oscillation. This problem is discussed in a paper from Van der Hagen et al. [112] using data from a Ringhals 1 measurement in 1990.

If one compares the phases and amplitudes of the global MATSTAB solutions with the mea-

surements (Figures 6.34-6.38), the good agreement supports the assumption, that the reactor was oscillating in the global mode. As in the Forsmark cases, the phase is predicted more accurate than the amplitude.

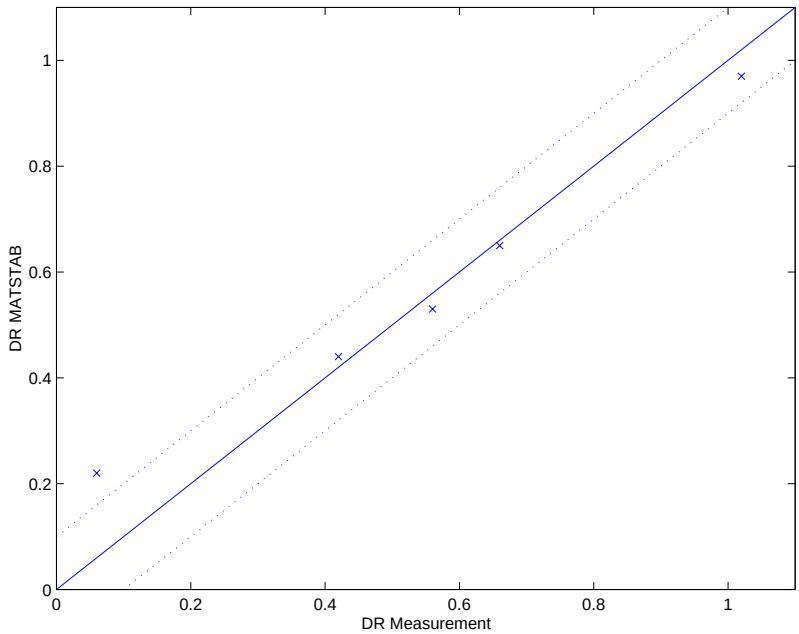

Figure 6.32: Validation of the Decay Ratio for Leibstadt Cycle 10

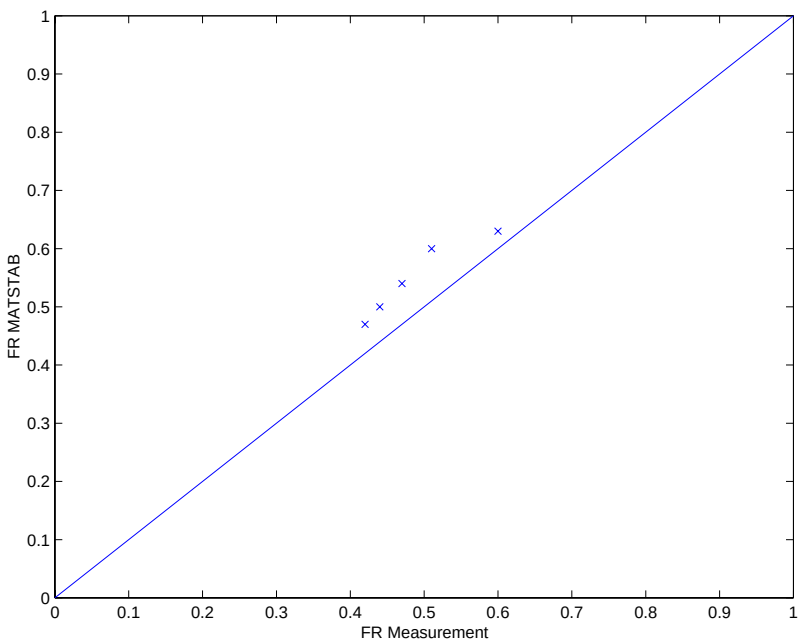

Figure 6.33: Validation of the Frequency for Leibstadt Cycle 10

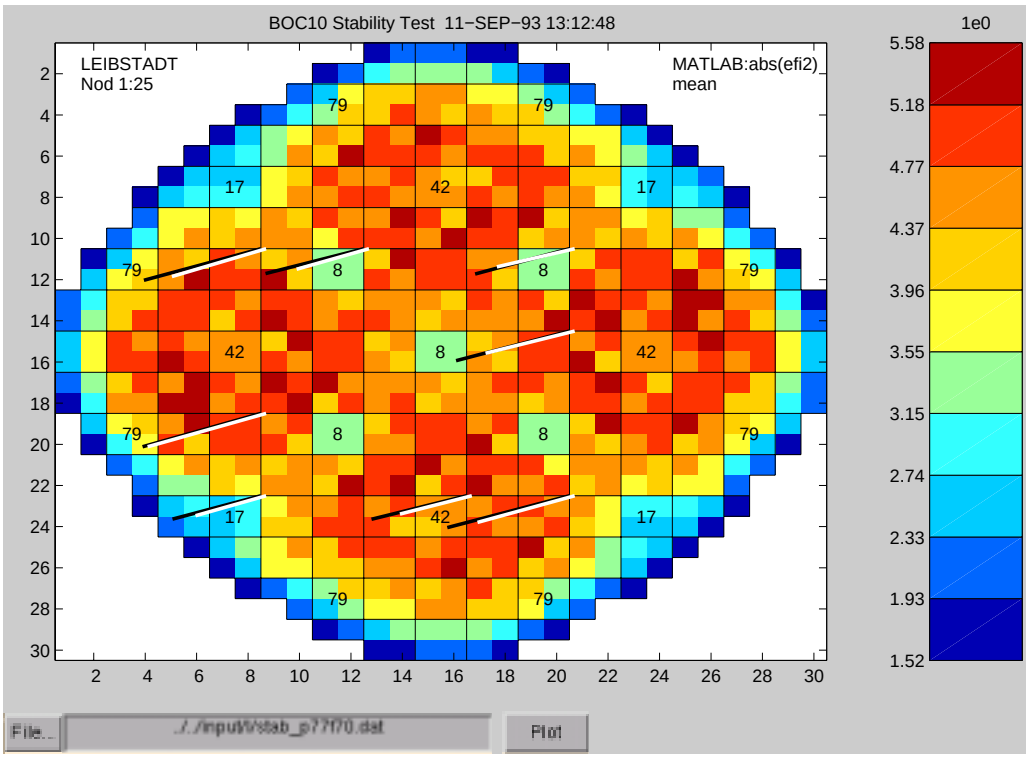

Figure 6.34: Comparison of MATSTAB and Measurement Point P77F70 in Leibstadt

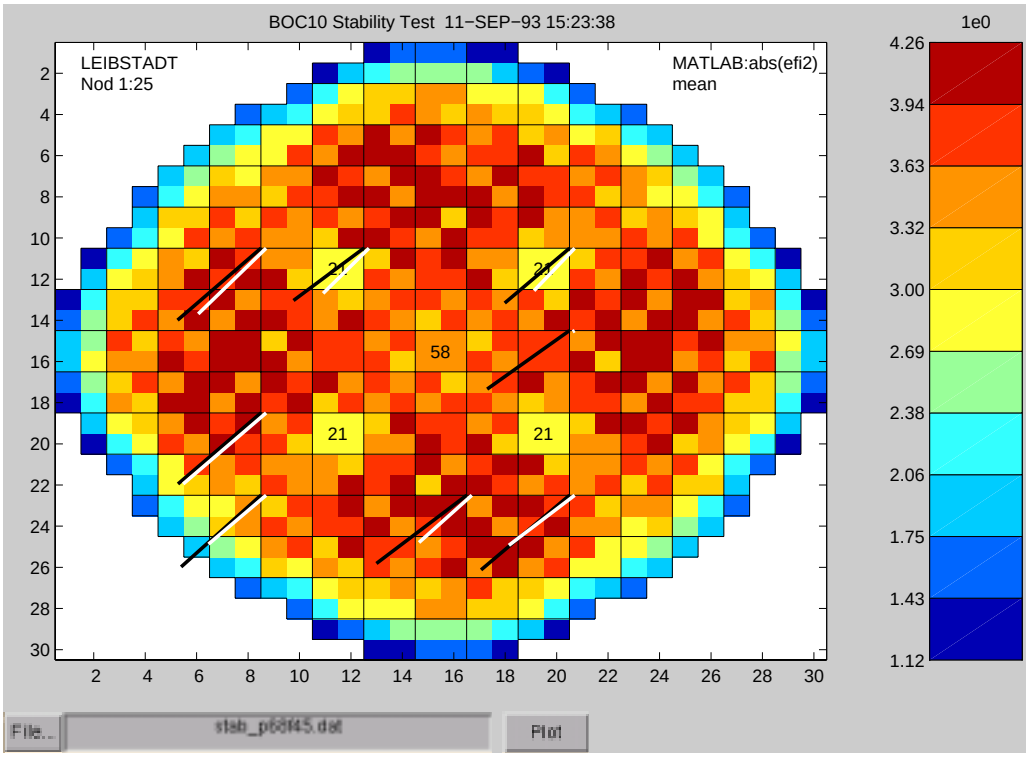

Figure 6.35: Comparison of MATSTAB and Measurement Point P68F45 in Leibstadt

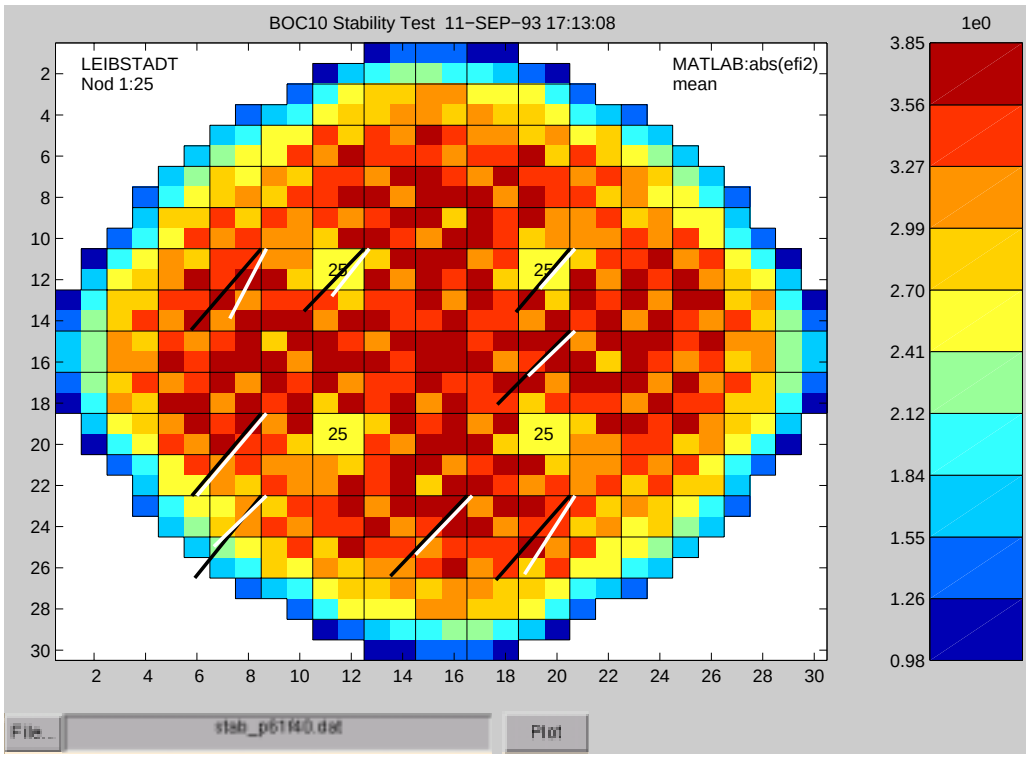

Figure 6.36: Comparison of MATSTAB and Measurement Point P61F40 in Leibstadt

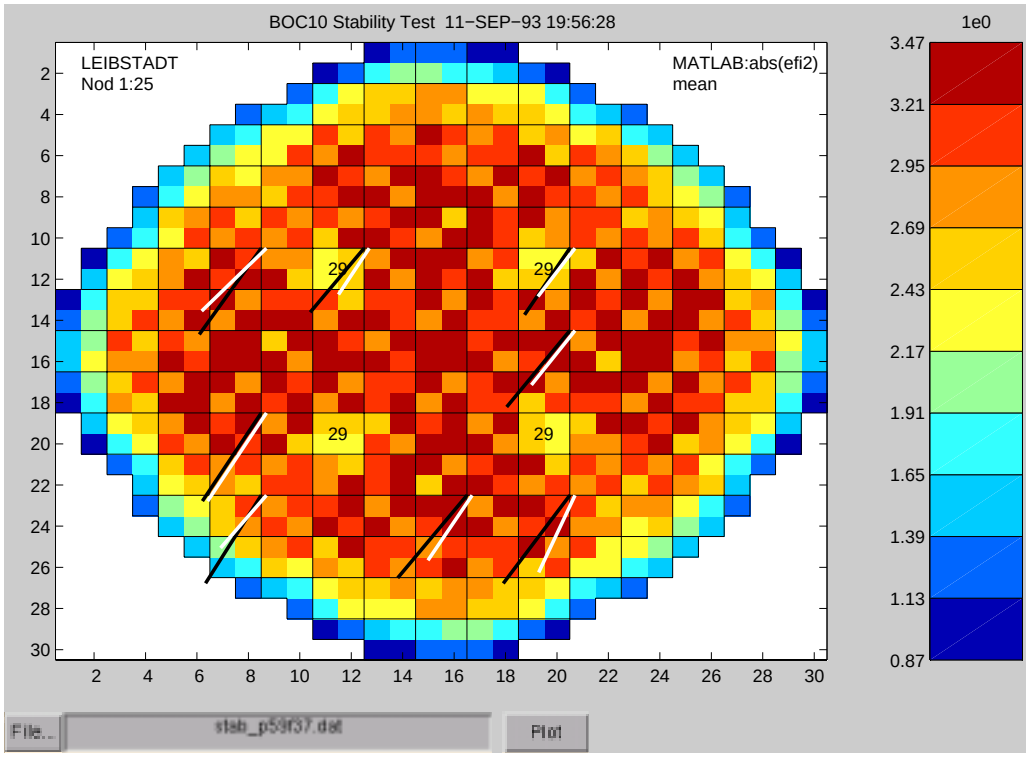

Figure 6.37: Comparison of MATSTAB and Measurement Point P59F37 in Leibstadt

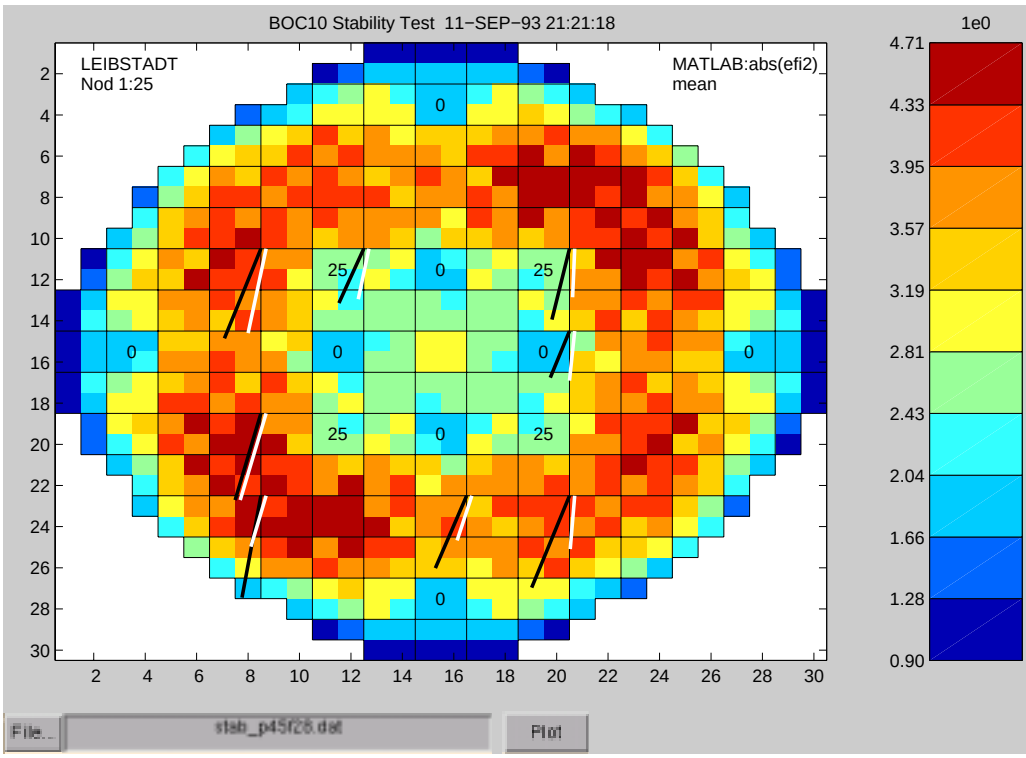

Figure 6.38: Comparison of MATSTAB and Measurement Point P45F28 in Leibstadt

6.3 Regional Oscillations

The ability to foresee regional oscillations, despite all the simplifications needed for a fast frequency-domain code, is one of MATSTABs big advantages. However, the MATSTAB module that deals with regional oscillations is not tested and validated as thoroughly as the global module. In addition, there are not many measurement cases available with dominating regional oscillations. A further problem is, that MATSTAB, as all linear codes, is not able to predict amplitudes.

MATSTAB only analyzes one operating point, therefore, the input data concerning the actual plant status is absolutely crucial for the results of the calculation. After a stability measurement, several hundred POLCA calculations are done to follow the operating points from startup to the measurement. This assures, that the xenon density and other time dependent quantities are taken correctly into consideration. The measurement itself, should be performed at a fixed operating point, which can be described by a POLCA steady state calculation.

If dominating regional oscillations occur, they can also interact with the global mode. For example, it is possible that within a few minutes, or even seconds, the oscillation pattern changes from global to regional and back again. To complicate things even further, the axis of

the regional oscillation may rotate in time. This behavior may take place while the operating point does not change significantly in power and core flow.

Therefore, MATSTAB cannot describe what happened during a measurement. However, MATSTAB can predict for a special operating point if regional oscillations are to be expected. MATSTAB is able to calculate not only the eigenvalue and hence the decay ratio for the global case, but also for as many regional oscillations modes as specified. If the decay ratio of a regional case is close to or even larger than the global one, regional oscillations are to be expected.

This simple and obvious rule was verified for all the Forsmark measurements, where the decay ratio of the regional case was always clearly smaller than for the global case.

6.3.1 Leibstadt

Things were very different in the case of Leibstadt during the measurements conducted in 1990 (cycle seven). The operating conditions were much less stable than in any Forsmark measurement. During the measurements of cycle seven, regional oscillations were actually observed, and a comprehensive report about the measurements series was written by J. Blomstrand [12].

Operating point			Decay Ratio			Frequency [Hz]		
Cycle	Power [%]	Core Flow [Kg/s]	Measurement	MATSTAB Global	MATSTAB Regional	Measurement	MATSTAB Global	MATSTAB Regional
C7	61.4	8466	0.20			0.53		
C7	55.2	4071	0.60/0.65	0.24	0.31	0.38/0.49	0.33	0.41
C7	56.9	4077	0.92-0.99	0.36	0.58	0.58	0.43	0.48
C7	58.6	4092	0.94-0.99	0.35	0.59	0.58	0.43	0.48
C7	58.6	4087	0.99-1.01	0.44	0.61	0.58	0.47	0.48
C7	58.6	4082	1.01-1.04	0.46	0.69	0.58	0.47	0.52
C7	58.0	4066	0.96-0.99	0.44	0.61	0.58	0.47	0.48

Table 6.7: Comparison Between MATSTAB and Measurements for Leibstadt Cycle 7

For the last five operating points, MATSTAB correctly predicts the domination of the regional oscillation (55.2/4071 was actually in phase). The decay ratio of the first regional mode is clearly larger than the decay ratio of the global mode (see table 6.7). The specific values of the decay ratios are, however, completely wrong for the global as well as for the regional case. The MATSTAB model of Leibstadt must be more or less correct, since it predicts good results for cycle 10. A mistake in the regional module would explain the small

values for the corresponding decay ratios, but could not explain the small values in the global case, because the global module is independent from the regional module.

The most likely cause for the large deviation between calculation and measurement is a mistake in the POLCA steady state. This assumption is supported by the fact, that not only the decay ratio, but also the frequency of the oscillation differs from the measurement. Since on one hand, the frequency is easy to predict, and on the other hand, the frequency is related to the transport time of the coolant through the core, POLCA most probably calculated a wrong steady state.

The mistake is systematically repeated in all operating points, as may be seen from the Figures 6.39 and 6.40.

There is no big surprise in the fact, that the phasor plots in Figure 6.41ff show also a large disagreement between calculation and measurement.

The only way to clarify the situation, as well as the reliability of MATSTAB for regional oscillations, will be the analysis of some regional measurements from another plant.

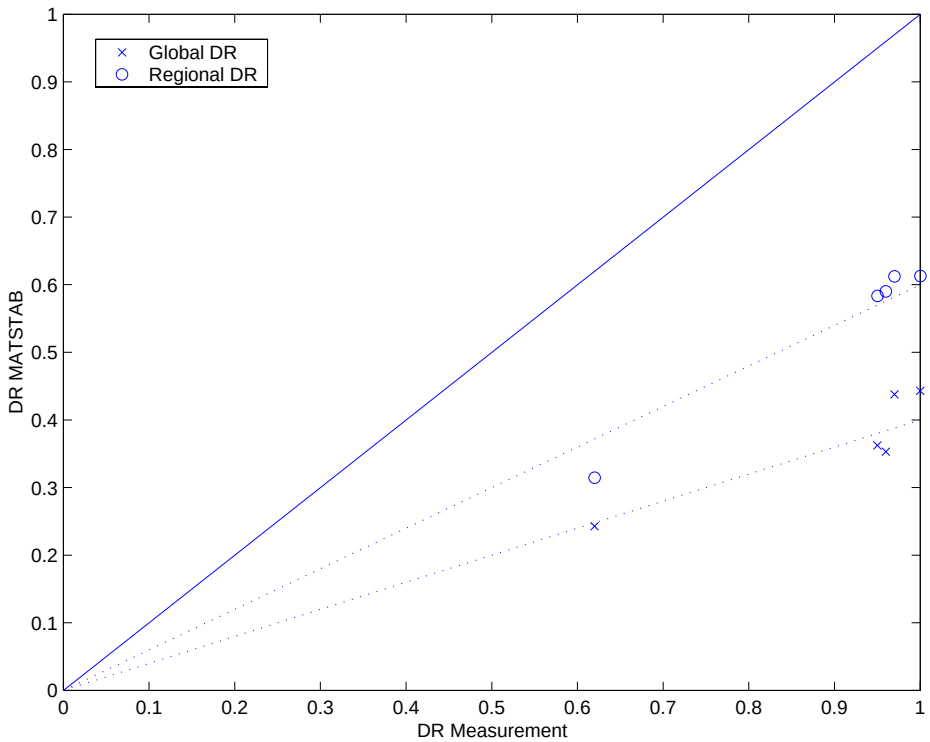

Figure 6.39: Validation of the Decay Ratio for Leibstadt Cycle 7

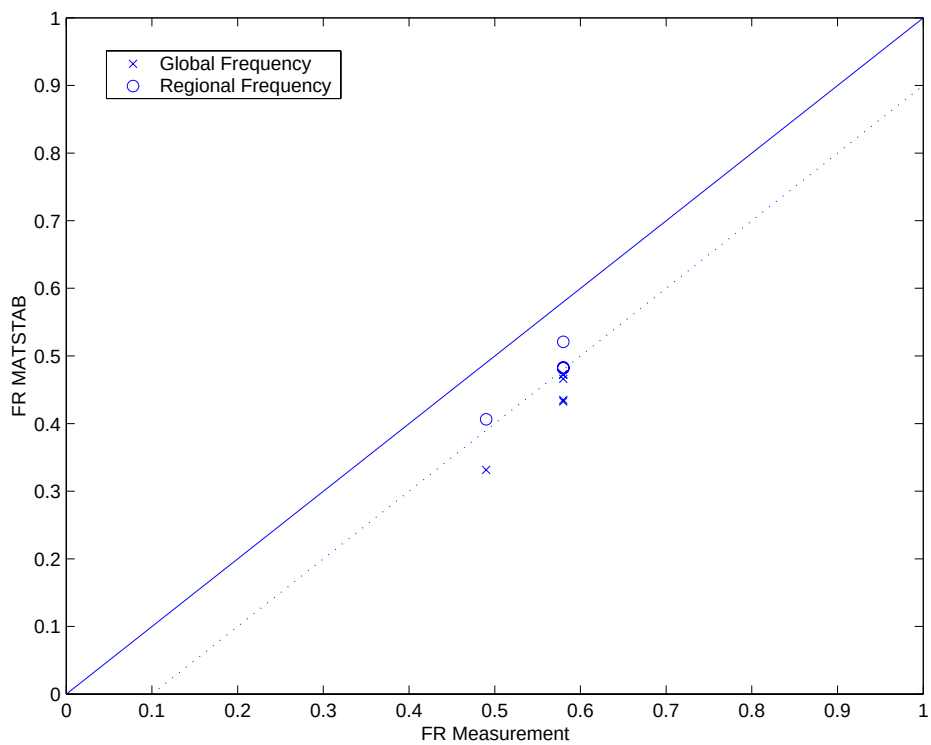

Figure 6.40: Validation of the Frequency for Leibstadt Cycle 7

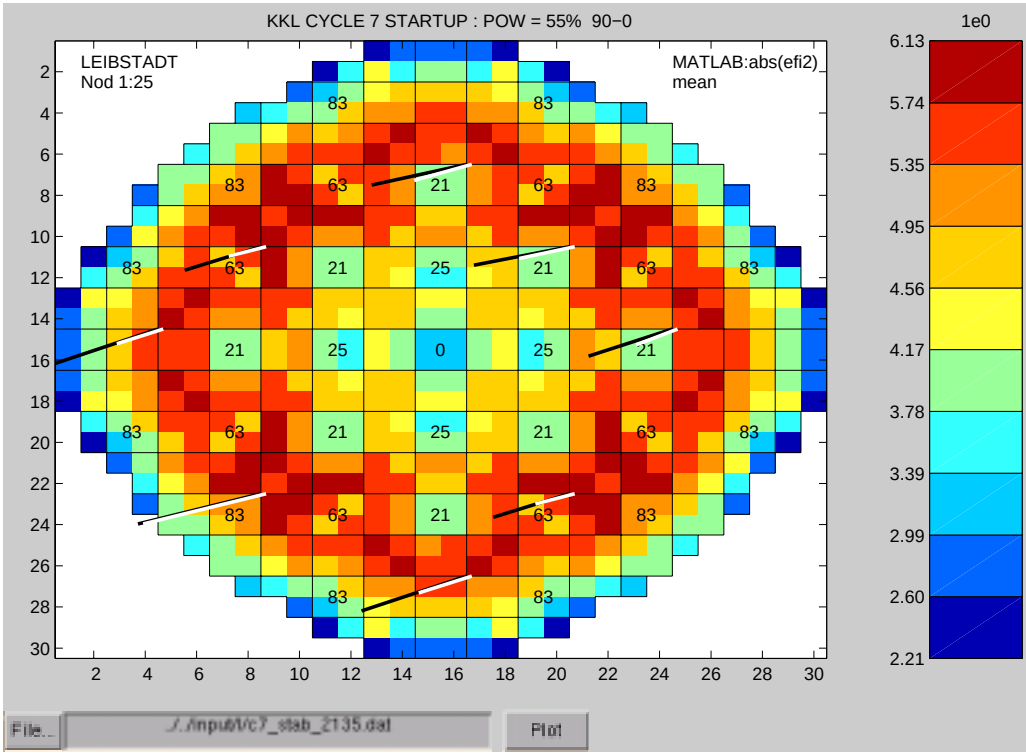

Figure 6.41: Comparison of MATSTAB and Measurement Point 21:35 in Leibstadt

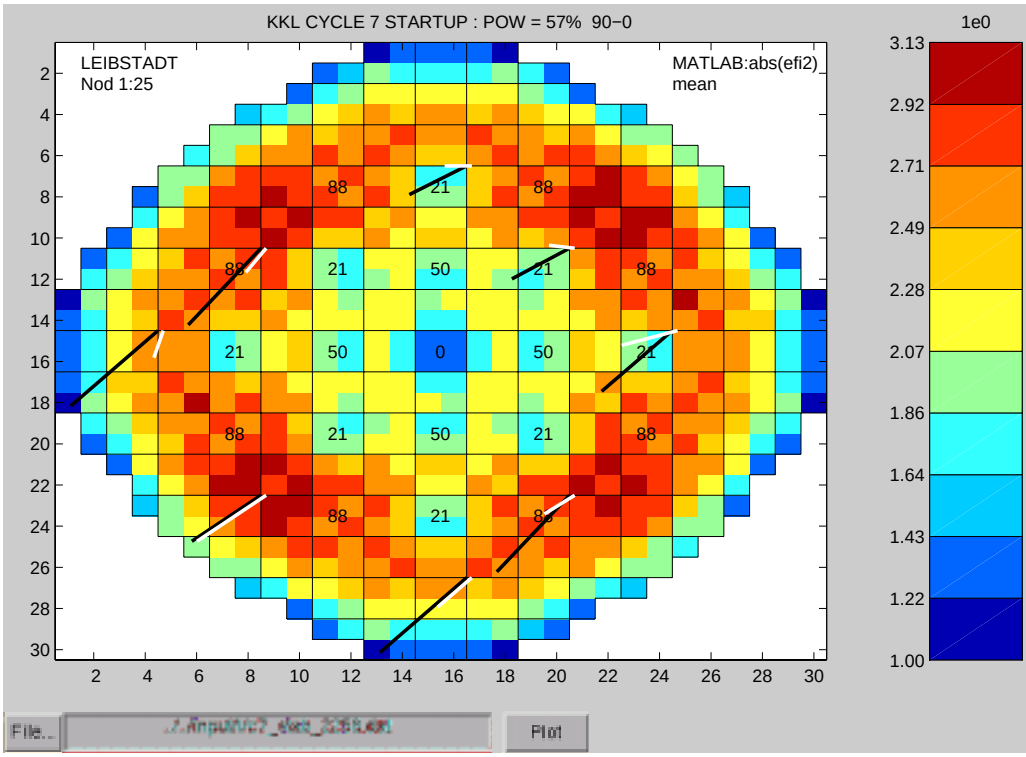

Figure 6.42: Comparison of MATSTAB and Measurement Point 22:58 in Leibstadt

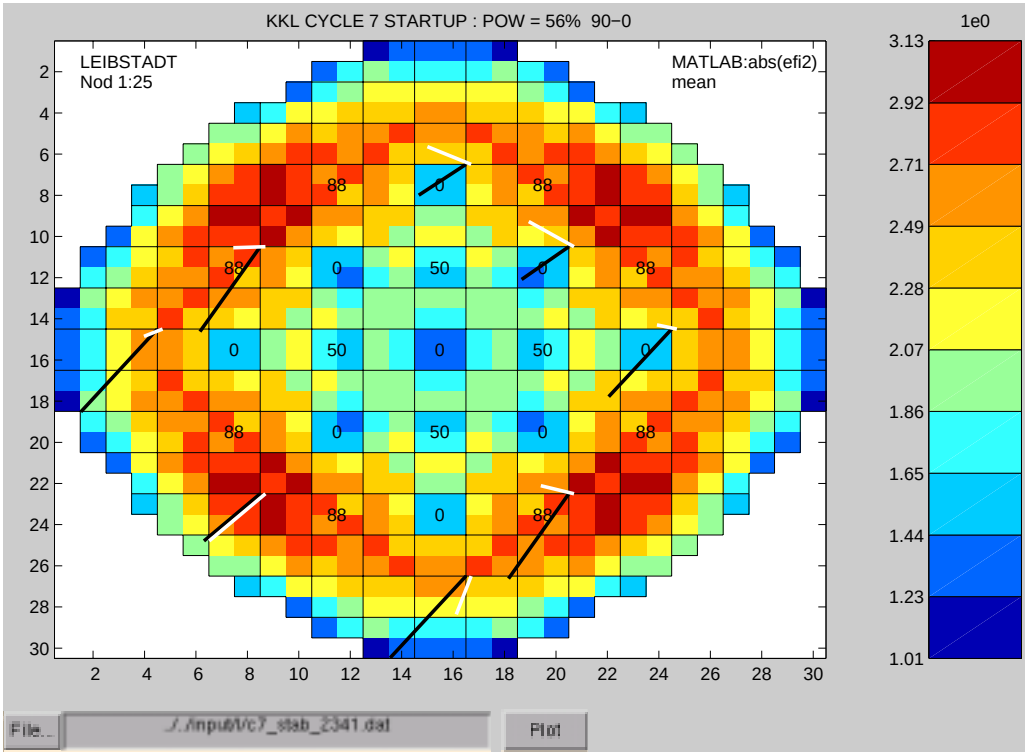

Figure 6.43: Comparison of MATSTAB and Measurement Point 23:41 in Leibstadt